Published in final edited form as:

Neurochem Res. 2022 January ; 47(1): 37–60. doi:10.1007/s11064-021-03299-w.

Serotonin Transporter Ala276 Mouse: Novel Model to Assess the Neurochemical and Behavioral Impact of Thr276 Phosphorylation *In Vivo*

Carina Meinke[1,2,*], **Meagan A. Quinlan**[2,*,#], **Krista C. Paffenroth**[3], **Fiona E. Harrison**[4], **Cristina Fenollar-Ferrer**[5], **Rania M. Katamish**[2], **Isabel Stillman**[2], **Sammanda Ramamoorthy**[6], **Randy D. Blakely**[2,7]

[1]International Max Planck Research School for Brain and Behavior, Max Planck Florida Institute for Neuroscience, Jupiter, FL USA

[2]Department of Biomedical Science, Charles E. Schmidt College of Medicine, Florida Atlantic University, Jupiter, FL USA

[3]Department of Pharmacology, Vanderbilt University, Nashville, TN, USA

[4]Department of Medicine, Vanderbilt University School of Medicine, Nashville, TN USA

[5]Laboratories of Molecular Genetics and Molecular Biology, National Institute on Deafness and Other Communication Disorders, National Institutes of Health, Bethesda, MD, USA

[6]Department of Pharmacology, Virginia Commonwealth University, Richmond, VA USA

[7]Florida Atlantic University Brain Institute, Jupiter, FL USA.

Abstract

The serotonin (5-HT) transporter (SERT) is a key regulator of 5-HT signaling and is a major target for antidepressants and psychostimulants. Human SERT coding variants have been identified in subjects with obsessive-compulsive disorder (OCD) and autism spectrum disorder (ASD) that impact transporter phosphorylation, cell surface trafficking and/or conformational dynamics. Prior to an initial description of a novel mouse line expressing the non-phosphorylatable SERT substitution Thr276Ala, we review efforts made to elucidate the structure and conformational dynamics of SERT with a focus on research implicating phosphorylation at Thr276 as a determinant of SERT conformational dynamics. Using the high-resolution structure of human

Correspondence: Randy D. Blakely, Ph.D., FAU Brain Institute, Rm 109, MC-17, 5353 Parkside Dr., Jupiter, FL 35348, rblakely@health.fau.edu.

*CM and MAQ contributed equally to the report

#present address: Department of Psychiatry and Behavioral Sciences, University of Washington, Seattle, WA, United States

Authors' contributions: CM and MAQ prepared data and figures and drafted the manuscript, MAQ evaluated SERT mRNA, protein levels and uptake kinetics and conducted analysis of data, KCP and FEH performed behavioral experiments and conducted analysis of data, CF-F generated and evaluated SERT structural models, RMK evaluated SERT protein levels and supported general aspects of the project, RDB and SR designed the Ala276 mouse line. All authors contributed to reviewing, editing and revision of the manuscript.

Conflicts of Interest/Competing Interests: The authors have no conflict of interest or competing interests to declare.

Ethics approval: Research with animals was reviewed and approved by the Institutional Animal Care and Use Committees (IACUC) of Vanderbilt University and Florida Atlantic University.

Availability of data and material: The datasets generated during and/or analyzed during the current study and the SERT Ala276 animal model are available from the corresponding author on reasonable request.

SERT in inward- and outward-facing conformations, we explore the conformation dependence of SERT Thr276 exposure, with results suggesting that phosphorylation is likely restricted to an inward-facing conformation, consistent with prior biochemical studies. Assessment of genotypes from SERT/Ala276 heterozygous matings revealed a deviation from Mendelian expectations, with reduced numbers of Ala276 offspring, though no genotype differences were seen in growth or physical appearance. Similarly, no genotype differences were evident in midbrain or hippocampal 5-HT levels, midbrain and hippocampal SERT mRNA or midbrain protein levels, nor in midbrain synaptosomal 5-HT uptake kinetics. Behaviorally, SERT Ala276 homozygotes appeared normal in measures of anxiety and antidepressant-sensitive stress coping behavior. However, these mice displayed sex-dependent alterations in repetitive and social interactions, consistent with circuit-dependent requirements for Thr276 phosphorylation underlying these behaviors. Our findings indicate the utility of SERT Ala276 mice in evaluation of developmental, functional and behavioral consequences of regulatory SERT phosphorylation *in vivo*.

Keywords

serotonin; transporter; phosphorylation; PKG; transgenic mouse

I. Introduction

The serotonin (5-hydroxytryptamine, 5-HT) transporter (SERT) is a member of the neurotransmitter sodium symporter (NSS, SLC6) family [47], which also includes the dopamine (DAT), norepinephrine (NET), glycine (GLYT) and ɣ-aminobutyric acid (GABA) transporters (GAT). Pioneering work by Baruch Kanner on the purification, reconstitution and cloning of GATs, and for whom this work is dedicated, were highly impactful on the corresponding author's career and his motivation to join the small club of investigators tackling the structure, function, regulation and genetics of neurotransmitter transporters, including SERT.

In the central nervous system, presynaptic SERT is responsible for the Na^+/Cl^- dependent clearance of 5-HT from the extracellular space, resulting in return of the neurotransmitter to the cytoplasm of nerve terminals where it can be re-packaged into secretory vesicles or metabolized [3,15]. 5-HT signaling modulates a variety of behaviors including mood, appetite, aggression and sleep, with alterations of SERT-mediated uptake implicated in the pathologies of various neuropsychiatric disorders [6,14,20,49,54,63]. Not surprisingly, SERT is a major target of therapeutic drugs used in the treatment of neurobehavioral disorders with selective 5-HT reuptake inhibitors (SSRIs) commonly used for the treatment of depression, anxiety and obsessive-compulsive disorder (OCD) [4,24,32]. Below, we provide a short review of key findings related to transporter structure in general and SERT structure in particular that likely underlie aspects of SERT post-translational regulation, with an emphasis on cytoplasmic domains harboring key phosphorylation sites, including Thr276. This residue's phosphorylation and impact on transport function has generated our goal of precluding this capacity *in vivo*, leading to our generation of the Ala276 mouse.

Structural characterization of SLC6 transporters

A significant advance in the understanding of SERT structure and function arose with the cloning of rat, mouse and human transporter cDNAs [7,8,27]. An evaluation of the predicted protein sequences from these studies revealed a highly conserved protein of 630 amino acids that hydropathy analyses predicted comprised twelve transmembrane (TM) domains connected by five intracellular and six extracellular loops. The amino- and carboxy-termini were predicted to be intracellular and, including the linker between the fourth and fifth TM, to contain putative phosphorylation sites [5,96] that could contribute to posttranslational SERT regulation [29,39]. SERT also contains putative *N*-linked glycosylation sites in a large extracellular loop between the third and the fourth TM regions, a feature shared with monoamine neurotransmitter transporters DAT and NET [21]. Mutation of glycosylation sites leads to an increase in electrophoretic mobility which was similar to the mobility of non-glycosylated transporter proteins [21,25]. This result indicated that the predicted *N*-linked glycosylation sites were in fact utilized and, therefore, consistent with the prediction that extracellular loop (EL) 2 was extracellular [3,18,21]. Because transporters of the NSS family show a high level of sequence conservation and almost identical hydropathy profiles [Obata11,12] it is common to apply structural features to all transporters of the family. Studies with site-directed antibodies targeted to DAT [28] and NET [18] sequences confirmed these findings. Using this approach, the amino- and carboxy-terminal of human NET was also found only be detected in intact cells after membrane permeabilization, confirming that both amino- and carboxy-termini are located in the cytoplasm [23].

To more directly validate the structure of SERT and study structure-function relationships, Androutsellis-Theotokis et al [43] evaluated functional impact of targeting of cysteine (Cys) residues in intracellular and extracellular loops by Cys alkylating reagents. Engineered Cys residues located in amino and carboxy termini and the five predicted intracellular loops (IL) were found to only confer sensitivity to membrane impermeant methanethiosulfonate (MTS) reagents when the membrane was permeabilized, confirming the location of these Cys residues as cytoplasmic [43]. Such Cys accessibility studies not only contributed to confirming the topology of NSS family members, they also allowed for the prediction of conformational changes of the transporter induced by substrate or inhibitor binding [34,35,41,43] . Further, the pattern of MTS sensitivity of Cys modified sequences could be used to infer whether a region conformed to an α-helical structure, as was found for several transmembrane domains [30,76], as well as the second intracellular loop (IL2), which was also found to be a larger intracellular loop that initially predicted [56].

While these studies provided evidence of the likely topology of NSS family members, a quantum leap in our understanding of NSS transporter arose from the generation of a high-resolution crystal structure of the bacterial leucine transporter (LeuT) from *Aquifex aeolicus* [55]. The structure of LeuT revealed, as predicted, a structure of twelve α-helical TMs connected by multiple ELs and ILs and with both amino and carboxy termini located in the cytoplasm. Moreover, the crystal structure revealed that TMs1-5 form an inverted topological repeat with TM6 - TM10. Within this repeat, both TM1 and TM6 are interrupted in their α-helical structures halfway through the membrane (TM1a, TM1b and TM6a, TM6b) and harbor the highest concentration of conserved amino acid residues. The helices

comprising TM3 and TM8 lie near TM1 and TM6, respectively, with a tilt of approximately 50°, and harbor highly conserved residues that surround the unwound regions of TM1 and TM6 to comprise the binding sites for Na^+ and the leucine. The transporter state crystalized is one where substrate and ions are occluded from both external and internal compartments, consistent with capture of an intermediate conformational state of an alternating access transport mechanism. The symmetry of the helices TM1 - TM5 and their corresponding inverted TM6 - TM10 helices in LeuT suggested a mechanism where rearrangement of these structural elements allow permeation of substrates from extracellular to cytoplasmic sides [55].

The crystal structure of LeuT together with site-directed modifications of SERT provided the basis for a model of alternating access that allow NSSs to transport their substrate [61,69,71] – “the rocking bundle” mechanism of transport [73]. In this model, the transport of neurotransmitter across the membrane bilayer requires a conformational change to cycle from an outward open state, in which the substrate binds to the transporter, to an inward open state, where the substrate can be released into the cytoplasm [73]. The major conformational change involves the tilting of a four-helix bundle consisting of TM1, TM2, TM6 and TM7 that surround the core of the substrate and ion binding site. Rocking of this four-helix bundle alternately moves the transporter from an inward occluded/ outward open state to an inward open/ outward occluded state. Cys accessibility data of rat SERT predicted that residues in TM1a, TM5, TM6b and TM8 become solvent accessible in the inward open conformation and form the cytoplasmic vestibule [56,61]. Each helix is the corresponding counterpart of the topologically inverted helices TM1b, TM10, TM6a and TM3 that contribute to the extracellular vestibule in the outward open conformation. This suggests a collapse of the opposite vestibule by opening and closing the extracellular or cytoplasmic permeation pathway due to the rotation of the four-helix bundle around the axis of the substrate and ion binding site [69,73]. The availability of LeuT structures in outward-open and inward-open states confirmed the alternating access mechanism, though with some refinements in structural movements. Analyses of the inward-open state suggested that only a part of the four helices moves as a unit and that the conformational change from outward-open to inward-open also requires independent movements of individual TM helices, including the tilt of TM1a and a rotation of TM6b. This same work also confirmed that the structural adjustments to open the intracellular gate are simultaneously ensuring the closure of the extracellular gate. Thereby, the large tilt of TM1a requires the TM5 helix to move which, in turn, forces TM7 and TM1b together resulting in the closure of the extracellular gate.

Amino and carboxy termini of NSS family are important for transporter regulation

With the cloning of NSS transporters and elucidation of cytoplasmically facing domains, substantial effort has been made to connect transporter function, trafficking, and regulation to these elements. Multiple consensus phosphorylation sites are evident in cytoplasmic domains [7,9] with most of the canonical serine (Ser) and threonine (Thr) phosphorylation sites being located in the amino and carboxy termini [36]. The SERT carboxy terminus has several potential recognition sites for protein kinase C (PKC), which is potentially involved in regulating protein–protein interactions with scaffolding proteins [53,58], and

mitogen-activated protein kinases (MAPK) such as p38 MAPK [91]. In contrast, SNARE protein syntaxin 1A [44] and calcium calmodulin-dependent protein kinase II (CaMKII) [91] most likely interact with N-terminal domains. The amino terminus and/or its interactors have been proposed to be involved in conformational changes that are required to support the transport cycle, since tethering of this sequence to the plasma membrane abolishes amphetamine-induced DA efflux [77] as does mutation of N-termimal Ser and Thr residues in DAT [48,84,98]. Because N- and C-termini are flexible transporter segments it has proven challenging to resolve these domains in a crystal structure. As a result, computational modeling and Fluorescence Resonance Energy Transfer (FRET) measurements have been used in an effort to gain additional insights in the role of the N- and C-termini in conformational dynamics and transporter regulation via kinases [89]. Computational models of SERT indicate two potential helices in the N-terminal domain and one region containing a helical element in the C terminus immediately after TM12. These results were further supported by FRET studies showing that insertion of proline residues within the predicted helices was not tolerated since they caused significant changes in FRET efficiency indicative of helix destabilization. Analyses of the terminal positions in outward-open and inward-open states showed a significant shift of the N-terminus as a consequence of transport-related conformational changes. These authors suggested that the terminal domains might interact with each other in SERT an outward-open state. However, the distance between the domains increased with the transition to an inward-open state making interactions less likely. On the other hand, the increased distance may allow the termini to be accessible for regulatory protein-protein interactions that only become possible in the inward-open state [89]. It is also possible that phosphorylation of the C terminus via kinases could alter its conformation and accessibility to allow interactions with other cytoplasmic domains to modulate transporter activity [88].

SERT function and 5-HT transport capacity is modulated by phosphorylation in response to activation of kinase pathways

As mentioned previously, the sequences of NSS family exhibited several potential phosphorylation sites leading to investigations into the role of multiple kinases and phosphatases in regulation of transporter activity [14,19,26,33]. Early on, researchers demonstrated that activation of protein kinases C (PKC) [31], A (PKA) [26], and G (PKG) [19] as well as calcium calmodulin-dependent protein kinase II (CaMKII) [17] acutely regulate SERT transporter activity and/or trafficking *in vitro,* potentially by direct phosphorylation. SERT was subsequently shown to be phosphorylated in parallel with regulation by endogenous protein kinases and phosphatases [36]. Thus, treatment of HEK-293 cells stably expressing human SERT (hSERT) with the PKC activator phorbol 12-myristate 13-acetate (PMA) lead to a significantly increased incorporation of radiolabeled phosphate in hSERT. In addition, PMA treatment simultaneously resulted in a dose-dependent decrease in 5-HT uptake [36] most likely due to reduced SERT surface expression [31]. SERT phosphorylation and loss of 5-HT uptake could be completely blocked by PKC inhibitors staurosporine and bisindolylmaleimide. It was further established that protein phosphatase PP1/PP2A inhibition promoted increased SERT phosphorylation and reduced uptake [36]. Intriguingly, PP2A and PKC act through distinct pathways as demonstrated by additive increases in hSERT phosphorylation following co-application of PKC activators and

PP2A inhibitors [36], suggesting the presence of PP2A-sensitive, SERT phosphophorylation sites targeted by other kinases. Interestingly, PKC-induced hSERT phosphorylation and sequestration were diminished in transfected HEK-293 cells in the presence of 5-HT or other SERT substrates such as fenfluramine [37]. This effect could be prevented by addition of SERT antagonists or by substitution of Na^+ and Cl^- which are required for 5-HT transport. These results indicate that surface expression of the transporter might be linked to activity state or, alternatively, that the presence of SERT substrates may alter the conformational state such that phosphorylation sites for PKC are not exposed [37]. In an attempt to elucidate the mechanism by which PKC modulates SERT activity, the time course of SERT phosphorylation, possible phosphorylation sites, and SERT trafficking events were investigated. A study by Jayanthi et al. [51] revealed a biphasic regulation of native SERT in rat platelets after PKC activation with PMA. In the first few minutes, PKC activation reduced SERT activity in a trafficking-independent manner by showing a reduction in V_{max} and a decreased affinity for 5-HT. Biotinylation studies further demonstrated no change in surface expression after five-minute exposure to PMA which indicates that the reduction in SERT activity results from an altered catalytic activity. However, a prolonged incubation time with the PKC activator caused a reduction in V_{max} with enhanced endocytosis of surface SERT. Consistent with different mechanisms underlying the biphasic kinetics of regulation, only Ser residues were phosphorylated within the first five minutes of PKC activation, whereas Thr residues were labeled after 30 min of PMA incubation. These results suggest that phosphorylation of Ser residues might drive reduced 5-HT uptake kinetics whereas more enduring phosphorylation of Thr residues, possibly by other kinases, might trigger SERT internalization [51].

In addition to PKC, activation of PKG in transfected cells also led to a significant increase of hSERT phosphorylation levels [36]. With respect to functional changes in native SERT, a study by Miller et al. [19] demonstrated that stimulation of adenosine receptors (AR) triggers an increase in SERT activity through a cGMP-linked pathway. SERT expressing rat basophilic leukemia cells (RBL2H3) were treated with 5’-N-carboxamidoadenosin (NECA), an AR agonist, resulting in increased 5-HT transport. This stimulation could be mimicked by treatment with the cell permeant cGMP analog 8-Br-cGMP, and the increase in 5-HT uptake induced by NECA could be completely blocked by the PKG inhibitor H8 [19]. Consistent with this result, subsequent studies provided evidence for a PKG-dependent signaling pathway that results in both a catalytic activation and trafficking of SERT upon activation of ARs [50]. In order to identify the signaling pathways that lead to AR-stimulated upregulation of SERT, RBL2H3 and transfected Chinese hamster ovary (CHO) cells were treated with multiple activators and inhibitors of phospholipase C (PLC), guanyl cyclase (GC), PKG and p38 MAPK. This work elucidated a signaling pathway in which activation of AR results sequentially in stimulation of PLC, followed by an increase in cytosolic Ca^{2+}, stimulation of nitric oxide synthase (NOS) and production of NO. The resulting GC activation results in cGMP production and activation of PKG. Notably, preventing cGMP hydrolysis by inhibiting PDE5 with sildenafil also resulted in a dose-dependent increase in 5-HT uptake that was additive with co-applied NECA. Radioligand binding assays further demonstrated that AR stimulation and PKG activation result in increased SERT surface density that arises from increased insertion and not from decreases in endocytosis, thereby

providing evidence for a trafficking-dependent mode of SERT regulation [50]. Subsequent biotinylation assays in hSERT-transfected HeLa cells confirmed this finding as 8-Br-cGMP treated cells also displayed elevated surface density of SERT [52]. In contrast, Ramamoorthy et al. [65] did not see an increase in SERT surface expression in his biotinylation studies when rat midbrain synaptosomes where treated with 8-Br-cGMP, even though 5-HT uptake was increased. Zhang et al. [100] also reported an increase in 5-HT uptake and SERT phosphorylation with no increase in SERT surface density in RBL2H3 cells when stimulated with NECA and cGMP using biotinylation of surface proteins. This discrepancy might relate to a PKG-dependent activation of p38 MAPK that leads in turn to catalytic activation of SERT [50], and where dominance of trafficking versus catalytic activation results from differences in incubation conditions or SERT expression levels. Indeed, stimulation of ARs with NECA resulted in significantly increased p38 MAPK phosphorylation that were mimicked by treatment of cells with the p38 MAPK activator anisomycin. Interestingly, pretreatment of the cells with the p38 MAPK inhibitor SB203580 prevented the increase in 5-HT uptake of NECA and 8-Br-cGMP. In contrast, SB203580 did not block the elevation in SERT surface density after NECA stimulation. These authors proposed that activation of the PKG pathway modulates SERT trafficking events and in parallel activates p38 MAPK which modulates catalytic activation of surface-resident SERT proteins [50]. Consistent with these data, several studies have shown that the increase in 5-HT uptake after direct stimulation of p38 MAPK with anisomycin reflects a reduction in K_m, but no change in V_{max} or SERT surface expression [52,57,62,74]. Another study monitored Qdot-labeled SERT proteins that are endogenously expressed in RN46A cells to demonstrate that treatment with 8-Br-cGMP increased SERT mobility by altering velocity and diffusion rates though the transporter is still constrained in membrane microdomains [82]. This result is consistent with a capacity of PKG to modulate surface SERT proteins independent of trafficking to the plasma membrane cytoplasmic SERTs are unlabeled in this approach. Finally, the increase in SERT instantaneous velocity detected after 8-Br-cGMP treatment was attenuated by co-incubating cells with the p38 MAPK inhibitor SB203580 indicating that a change in SERT initiated by PKG activation can be transmitted to SERT or its regulatory partners through p38 MAPK. After investigating SERT-cytoskeletal interactions, the authors suggested that the elevation in catalytic activity might result from relaxed cytoskeletal tethering following PKG/p38 MAPK activation which allows SERT to adopt conformations that support increased transporter activity [82].

Thr276 site dictates PKG-dependent SERT regulation

The studies noted above provided evidence that PKG pathway activation leads to increased 5-HT transport. The simplest explanation for kinase-dependent transporter regulation would be via direct PKG-mediated SERT phosphorylation. In an effort to explore this possibility, Ramamoorthy et al. [65] provided the first evidence for a specific SERT phosphorylation site – Thr276. Using rat midbrain synaptosomes, these investigators reported an increase in ^{32}P incorporation as well as enhanced 5-HT uptake when synaptosomes were treated with 8-Br-cGMP. Both effects were effectively blocked by different PKG inhibitors, but not by inhibitors of PKA or PKC. Phosphoamino acid analyses provided evidence that PKG activation leads to phosphorylation of Thr residues. After individually mutating eighteen human SERT (hSERT) Thr residues to Ala, only the Thr276Ala substitution

in the second IL blocked stimulation of 5-HT uptake and SERT phosphorylation after 8-Br-cGMP stimulation, providing the first direct link between SERT phosphorylation and 5-HT transport in response to PKG activation. Importantly, the hSERT Ala276 mutant still exhibited wildtype (WT) 5-HT uptake levels under basal conditions. To support a direct phosphorylation of SERT at 276 can solely account for transport enhancement, the investigators substituted Thr with aspartic acid (Asp) and found that levels of 5-HT uptake in SERT Asp276 transfected cells was comparable to the levels achieved with WT-hSERT (Thr276) transfected cells treated with 8-Br-cGMP. Moreover, treatment of hSERT Asp276 transfected cells with 8-Br-cGMP did not further enhance 5-HT uptake, as expected if Thr276 is the sole, essential phosphorylation site involved in PKG-dependent SERT regulation [65].

Our group has provided evidence for a PKGIα-linked pathway in the elevation of SERT activity, including colocalization of native kinase and transporter in the rat serotonergic neuroblastoma RN46A, formation of a stable hSERT/PKGIa complex in co-transfected HEK-293T cells, suppression of 8-Br-cGMP stimulation of SERT activity in these cells by the PKGI-specific inhibitor DT-2, as well as elimination of hSERT activity stimulation in transfected HeLa cells by a PKGI specific siRNA, and formation of a stable PKGI/hSERT complex in co-transfected HEK 293T cells. Indeed, recent studies suggest that SERT may not be directly phosphorylated by PKGI [87,91,100]. A study by Wong et al. [87], however, has provided compelling evidence that SERT may not be a direct substrate of PKG. In a clever manipulation, these investigators utilized a PGK Iα mutant Met438Gly that utilizes a modified ATP analog for phosphorylation and found that the mutant was unable to phosphorylate SERT when cells were incubated with the labeled ATP analog. These findings suggest that PKG targets another kinase that phosphorylates SERT at Thr276 [87], reminiscent of the role played by p38 MAPK as a supporting pathway in SERT regulation following PKG activation. Sørensen et al. [91] generated peptides that correspond to cytoplasmic regions of SERT and performed *in vitro* phosphorylation using several kinases, followed by liquid chromatography-tandem mass spectrometry (LC-MS/MS) of these hSERT peptides to identify sites of phosphorylation [91]. One of these peptides represented the portion of IL2 containing Thr276, as well as Ser277, another potential phosphorylation site. Ser277 of this peptide was indeed phosphorylated, however, not by PKG, but by PKC. These findings should be interpreted cautiously as they 1) may not reflect the conformation of the peptide in the native transporter (in outward-facing or inward-facing conformations) and do not allow for a sequential action of kinases, for example of Ser phosphorylation by one kinase and Thr phosphorylation by the other, since a combination of kinases was not explored. Indeed, no hSERT segment was found to be phosphorylated by PKGI, consistent with the idea that the kinase does not phosphorylate SERT directly. Certainly, inferences from *in vitro* findings to the *in vivo* setting must be made cautiously, ours included. Recently, we used a proteomic approach to examine the composition of native SERT complexes in the mouse midbrain [108]. Whereas we found PKGII levels to be very level in RN46A cells. PKGII was identified in mSERT complexes by co-immunoprecipitation followed by mass spectrometry analysis. Additionally, the location of Thr276 in the small second intracellular loop between TM4 and TM5 raises questions as to its utilization given the likely restricted accessibility of this site to aqueous reagents.

Moreover, an α-helical character of the loop peptide might not be compatible with the binding of the kinase, at least in some conformations [56].

Structural basis for SERT activity enhancement by Thr276 phosphorylation

A potential mechanism of how the Thr276 site could still be phosphorylated was shown by the inward-open and outward-open X-ray structure MhsT, the NSS homolog of *Bacillus halodurans* [95]. The conformational change from outward- to the inward-open state demonstrated a partial unwinding of the cytoplasmic end of the TM5 helix. Thereby, the region containing Thr276 extends into the cytoplasm which if achieved in hSERT could potentially makes the Thr276 site accessible to kinases. Support for this mechanism has come from studies by the Rudnick laboratory who provided evidence for conformation-dependent phosphorylation of SERT Thr276 [100]. In addition to providing direct evidence that Thr276 is phosphorylated upon PKG activation through use of a phospho-Thr276 antibody, they showed that outward-open stabilizing agents such as Na^+ and cocaine decreased SERT phosphorylation at Thr276, whereas inward-open stabilizing agents such as the substrate itself 5-HT and ibogaine increased Thr276 phosphorylation. Extracellular Na^+ stabilizes the transporter in an outward-open state [89] waiting for 5-HT to bind which then leads to transport-induced conformational rearrangements to an inward-open state to release the substrate [61,81]. The presence of Na^+, cocaine, 5-HT and ibogaine had no noteworthy effects on kinase activity, indicating that the alterations in phosphorylation are most likely due to changes in SERT conformation. This idea is further supported by the observation that extracellular Cys404 was accessible in the presence of Na^+ indicating an outward-open conformation, whereas cytoplasmic Cys277 was accessible in the presence of ibogaine indicating an inward-open conformation. Thus, SERT conformation has an impact on phosphorylation of the transporter, with SERT being more susceptible to PKG-induced phosphorylation at Thr276 in an inward-facing conformation. These findings are reminiscent of those of Ramamoorthy and Blakely [37] who as noted above demonstrated that incubation of SERT expressing cells with 5-HT and other substrates, in a Na^+-dependent manner, precludes phosphorylation of SERT following stimulation of PKC.

With its proposed position at the cytoplasmic end of TM5, Thr276 is located in the cytoplasmic permeation pathway that is opening and closing due to structural adjustments in the different conformational states [73,85]. This aspect suggests that modification of Thr276 would be predicted to modify the kinetics of 5-HT transport as a consequence of altering SERT conformational dynamics. This possibility is supported by studies of the naturally occurring, hyperactive hSERT coding substitutions Ile425Val and Gly56Ala that are associated with OCD and ASD, respectively, and that are not further responsive to PKG and p38 MAPK activation [52]. The Val425 variant was found in patients with 5-HT-related neuropsychiatric disorders including OCD [46] and was investigated early on in regards of changes in 5-HT transport [45]. The variant demonstrated increased basal 5-HT uptake rates caused by a reduction in 5-HT K_M and an increase in V_{max}, though no change in SERT surface density could be observed. Interestingly, 5-HT uptake of hSERT Val425 could not be further increased by treatment with a NO generator or 8-Br-cGMP [45]. However, transport levels of this mutant were decreased to WT levels using a PKG inhibitor [67]. Another study by Prasad et al. [52] supported the insensitivity of hSERT Val425 to 8-Br-cGMP, although

they observed an increase in SERT surface density using biotinylation methods in contrast to earlier studies. This difference was previously discussed [75,96] with technical differences such as level of expression achieved by transfected cell host possibly playing a role in the discrepancy.

In addition to hSERT Val425, the ASD-associated substitution hSERT Gly56Ala was identified along with multiple other hSERT coding variants, including another activating substitution at position 425 (Ile425Leu). All but one of the ASD-associated hSERT variants, Ala56, are rare, found within single families. hSERT Ala56 on the other hand has an allele frequency of ~1% in the United States, with more than 30,000 individuals expected to be homozygous for the substitution [103]. Like hSERT Val425 (or Leu425) transfected cells, hSERT Ala56-transfected cells exhibited increased basal 5-HT transport activity with a reduction in 5-HT K_M, but with no change in V_{max}, and no change in SERT surface density, mirroring the elevation in catalytic activity that arises from acute p38 MAPK activation [52,62,74]. In addition to increased 5-HT uptake, the variant demonstrated a significantly elevated basal phosphorylation which cannot be further increased by treatments with 8-Br-cGMP [52]. After introducing SERT Gly56Ala into a mouse to investigate its impact *in vivo*, behavioral analyses revealed impaired social behavior and communication as well as abnormal repetitive behavior [86] which represent core deficits in ASD [38]. As predicted from *in vitro* studies, *in vivo* studies with SERT Ala56 mice revealed elevated hippocampal 5-HT clearance under basal conditions. *Ex vivo* studies with midbrain synaptosomes demonstrated hSERT hyperphosphorylation that could be normalized by inhibiting p38 MAPK activity [86]. These results indicate that constitutive phosphorylation triggered by the Ala56 mutation prevents the SERT variant from transitioning between high and low activity states. To further explore the role of p38 MAPK in mediating hyperactivity and hyperphosphorylation of the Ala56 variant *in vivo*, SERT Ala56 mice were injected with the p38α MAPK inhibitor MW150 once a day for five days. Remarkably, the inhibitor normalized the elevated 5-HT clearance rates. Further, conditional elimination of p38α MAPK in serotonergic neurons of Ala56 mice rescued behavioral phenotypes such as social withdrawal as assessed the tube test and normalized 5-HT receptor sensitivities [103]. Together, these studies suggest that the SERT Ala56 variant may exists constitutively in a conformation that is normally induced transiently by PKG [50] and/or p38 MAPK [50,57].

The SERT Gly56Ala substitution does not impact the sequence of a putative phosphorylation site. However, Gly56 is located in the amino terminus of SERT which has been shown to support protein associations [68,72]. Indeed, Quinlan and colleagues [108] have shown via proteomic studies that the SERT purified from mice expressing Ala56 vs Gly56 (WT) exhibit a significant reduction in SERT-associated proteins. Possibly, a substitution from Gly to Ala may cause a modification in the secondary structure of the amino terminus that limits association of, or restricts access by, protein phosphatases, thereby allowing enhanced kinase access to cytoplasmic phosphorylation sites. This could result in SERT Ala56 being biased toward an outward facing conformation with high affinity for 5-HT and without the ability to adapt to environmental changes that normally impose SERT regulation [86]. Quinlan et al. [107] provided evidence that the Gly56Ala substitution indeed causes a conformational alteration with the transporter being biased to an outward-open conformation. As mentioned earlier, it was proposed that N- and

C-termini interact when SERT is in an outward-open state with the distance between the terminal domains increasing when SERT transitions to the inward open state [89]. After transfecting cells with hSERT WT and Ala56 SERT constructs that are dually tagged with cyan fluorescent protein (CFP) on the N-terminus and yellow fluorescent protein (YFP) on the C-terminus, FRET measurements were performed to inspect the relative proximity of amino and carboxy termini. These studies revealed a significant increase in FRET efficiency with the C-Ala56-Y variant compared to WT C-SERT-Y, indicating greater proximity of N- and C-termini in the hSERT Ala56 variant, consistent with a biased open-outward state. Further, Cys substitutions in IL2 were less reactive to MTSEA in the Ala56 variant, whereas the reactivity of an extracellular facing Cys residue increased compared to that seen in WT hSERT. The results of this study support a model whereby SERT activating stimuli acting through cytoplasmic pathways, be they signal transduction networks or cytoplasmic facing domains, can bias the transporter to reside more frequently in an outward-open conformation. As mentioned before, Zhang et al. [100] demonstrated increased phosphorylation of Thr276 after PKG activation when SERT was stabilized in the inward-open state, which as this phosphorylation is stimulatory, must accelerate conformational transitions that support a rate-limiting step in the transport cycle.

Together, these studies link conformational bias to enhanced PKG and p38 MAPK-dependent activation of SERT, a protein whose altered activity has been associated with neuropsychiatric disease [45,52,74,86,103]. Although the functional significance of altered SERT protein phosphorylation and function has been made apparent by studies of engineered and naturally occurring coding variants, key issues remain unresolved, including how phosphorylation site accessibility varies as a function of conformational state, how changes in phosphorylation elicit elevated transport rates, and whether predictions from *in vitro* studies translate *in vivo*. In this report, we provide two contributions to these questions. One involves an inspection of the conformation-dependent exposure of the Thr276 residue via molecular modeling based on SERT structures locked in open-out and open-in conformation. The second brings to the fore our effort to establish the significance of SERT phosphorylation in general, and Thr276 specifically, *in vivo*.

II. Methods

Molecular modeling of SERT Th276

The structural model of the hSERT in an outward-facing conformation was obtained using the X-ray structure of outwards hSERT bound to s-citalopram (SERT-Cit) (PDB id: 5I71 [97]) as a template, which contains several thermostabilizing mutations named Y110A, I291A, T439S and alanine substitutions in the surface-exposed cysteines C554, C580 and C622. The sequence alignment between the amino acid sequences corresponding to the transmembrane domains of the SERT-Cit and the WT hSERT was obtained using ClustalW [22] and was used to create a pool of 2000 models using Modeller [16]. The final outwards WT hSERT model, that covers residues 77 to 616, was that with the best MODELLER score and best stereochemistry as per Procheck analysis [13]. The Solvent-Accessible Surface Area (SASA) per residue was calculated as the percentage of the SASA of a given residue X in the context of the tripeptide Gly-X-Gly using the method of Honig [10]. The radius

of the probe used to define the surface was 1.4 Å and a 30 Å thick layer of pseudo atoms was used to represent the membrane. The analysis regarding the inward-facing conformation of hSERT were performed on the CryoEM structure of the transporter bound to ibogaine (PDBid: 6dzz [105]). The phosphorylation of T276 of hSERT CryoEM in the inward-facing conformation was performed manually using Pymol software.

Creation of SERT Thr276Ala knock-in mice

All experiments using animal subjects were conducted according to the National Institutes of Health Guide for the Care and Use of Laboratory Animals and were preapproved by the Vanderbilt University and Florida Atlantic University Institutional Animal Care and Use Committees. To generate the SERT Ala276 knock-in (KI) mouse model, we utilized CRISPR/Cas9 technology. Briefly, by using the online CRISPR design software developed in the Zhang laboratory (Massachusetts Institute of Technology, http://crispr.mit.edu) we identified and generated oligos to insert our guide RNA (Sense RB5167: CACCGAGGAGTCAAAACGTCTGGCA; Antisense RB5216: AAACTGCCAGACG TTTTGACTCCTC) into pX330 (Addgene plasmid #42230) that also encodes SpCas9 enzyme. Donor oligos were also generated to generate a non-synonymous SNP that changes threonine (ACG) to alanine (GCG) at amino acid 276 (bolded and underlined below; RB5192: GCATCATGCTCATCTTCACCATTATCTACTTCAGCATCTGGAAAGGAGTCAAA**GCG** TC TGGCAAGTTGAGGACTCTGCAGCTTGTCCTGAACTGCCCAGGGCCCCGCAG). The plasmid and donor oligo were injected into C57BL6/J embryos through the Vanderbilt Gene Editing Resource. A founder heterozygous male mouse labeled #9 (Figure 2b) was bred with a C57Bl/6J female to produce pups that were verified to contain the intended mutation via sequencing and then were then backcrossed for 10 generations on a C57Bl/6J background to remove off target CRISPR events. For all experiments, we used male and female SERT Ala276 and SERT Thr276 (WT) littermates at 8-12 weeks old generated from heterozygous breedings. Mouse genotyping was conducted by Transnetyx, Inc. using real-time PCR (Slc6a4-10 MUT; Forward Primer: TGCAGATCCATCAGTCAAAGG; Reverse Primer: CCCTTGAACCTTCTAACAGATGTG).

Assessment of growth and Mendelian inheritance of SERT Ala276 mice

Assessment of genotype and sex distribution from all mice derived from heterozygous breeding were compared to the expectation derived from Hardy–Weinberg equilibrium using χ^2 tests set to $P < 0.05$ as a determinant of statistical significance. To assess growth of the animals from development to adulthood, both male and female mice of all three genotypes were weighed weekly from 4 to 10 weeks of age. Data were analyzed using a two-way repeat measure ANOVA to determine statistical significance across genotypes.

Irwin screen for physical, sensory and motor differences

An Irwin screen performed as described [1] was conducted to provide initial inspection of gross physical appearance, sensorimotor function and behavior. All examinations were performed blind to genotype. First, physical factors and gross appearance were recorded by: coat color, body weight, presence of whiskers (3 = a full set), appearance of fur (2 =

well groomed, normal), piloerection (0 = none, 1 = most hair standing on end); patches of missing fur on face and body (2 = extensive), wounds (4 = extensive). Next, mice were monitored and scored in a novel environment (3 minutes in a clean tub cage) by: transfer behavior (5 = no freeze, immediate movement), body position (4 = rearing on hind legs), spontaneous activity (0 = none, resting); respiration rate (2 = normal), tremor (2 = marked), palpebral closure (2 = eyes closed), piloerection (1 = coat stood on end), gait (0 = normal), pelvic elevation (2 = normal, 3mm elevation), tail elevation during forward motion (1 = horizontal extended), urination (1 = little), and defecation (number of fecal boli emitted during 3 minute period). Then, reflexes and reactions to simple stimuli were observed and scored by: touch escape (finger stroke from light to firm; 2 = moderate rapid response to light stroke), positional passivity (struggle response to sequential handling; 0 = struggles when restrained by tail), trunk curl (grip tail and lift about 30 cm; 1 = present), body tone (compress both sides of the mouse between thumb and index finger; 1 = slight resistance), and pinna reflex (while the mouse was gently restrained, the auditory meatus was lightly touched with the tip of a 31 gauge stainless-steel wire probe and ear retraction or head movement was recorded; 1 = active retraction, moderately brisk flick). Finally, during supine restrain, the following was scored: skin color (color gradations of plantar surface and digits of forelimbs, 1 = pink), heart rate (felt by palpation below sternum; 1 = normal), abdominal tone (palpation of abdomen, 1 = slightly resistance), and proved biting (gently inserted dowel between the teeth at the side of the mouse, 1 = present). Data from each measure were analyzed by the Kruskal-Wallis test.

Quantitative real-time PCR analysis of SERT mRNA expression

A quantitative real time polymerase chain reaction (qPCR) assay was utilized to determine midbrain and hippocampal *Slc6a4* (SERT) mRNA expression using SERT Thr276 (WT) and SERT Ala276 heterozygous and homozygous animals. Midbrain and hippocampus samples were collected from both male and female mice that were sacrificed by rapid decapitation, with tissues immediately frozen on dry ice, prior to storage at −80°C. RNA isolations were conducted from tissue samples using Trizol reagent (Thermo Fisher, Catalog no. 15596018) according to manufacturer's instructions. The total RNA concentration for each sample was quantified by spectrophotometry using the LVis plate (BMG LabTech, FLUOstar Omega Plate Reader, Omega Software Version 5.11) with the purity of samples checked to confirm that the 260/280 ratio was in the range of 1.8–2.1. Reverse Transcription was conducted on 1μg of RNA using a High Capacity cDNA Reverse Transcription Kit according the manufacturer's instructions (Applied Biosystems, Catalog no. 4368814). qPCR was conducted on the cDNA using a Taqman Gene Expression assay consisting of the Taqman Gene Expression Master Mix and appropriate Taqman probes (Master Max: Thermo Fisher Scientific, Applied Biosystems, Catalog no. 4369016, Taqman probes: *Slc6a4* Mm00439391_m1, Catalog no. 4331182; 18S HS99999901, Catalog no. 4331182). All experiments were conducted using a Bio-Rad qPCR machine (Bio-Rad CFX96 Real-Time System, C1000 Touch Thermal Cycler). Sample mRNA levels from qPCR assays were calculated using the ΔΔCt method [70] and normalized compared to WT littermates and the threshold cycle (Ct value) of each gene was then normalized to 18S rRNA expression. Data were analyzed using a one-way ANOVA to determine statistical significance across genotypes for each sex.

HPLC-based neurochemical analysis

Neurochemical measures were assessed in the Neurochemistry Core Facility at Vanderbilt operated by the Vanderbilt Brain Institute. Brain regions, harvested and dissected as noted above, were flash-frozen in liquid nitrogen and stored at −80°C. Frozen brain tissue was homogenized using a tissue dismembrator (Misonix XL-2000; Qsonica, LLC, Newtown, CT) in 100-750 μL of a solution containing 100 mM TCA, 10 mM $NaC_2H_3O_2$, 100 μM EDTA, 5 ng/mL isoproterenol (an internal standard), and 10.5% methanol (pH 3.8). Samples were spun in a microcentrifuge at 10000 *x g* for 20 min. and the supernatants were stored at −80°C until assayed (Cransac et al., 1996). Prior to assay, thawed supernatants were centrifuged at 10000 *x g* for 20 min. before being analyzed by HPLC. Twenty μL of each sample were injected using a Waters 2707 auto-sampler onto a Phenomenex Kintex (2.6 u, 100 A) C18 HPLC column (100 x 4.6 mm). Biogenic amines were eluted with a mobile phase (89.5% 100 mM TCA, 10 mM $NaC_2H_3O_2$, 100 μM EDTA, and 10.5% methanol (pH 3.8)) delivered at 0.6 mL/minute using a Waters 515 HPLC pump. Analytes were detected utilizing an Antec Decade II (oxidation: 0.4) (3 mm GC WE, HYREF) electrochemical detector operated at 33°C. HPLC instrument control and data acquisition was managed by Empower software. Amino acids were evaluated using a Waters AccQ-Tag system with a Waters 474 Scanning Fluorescence Detector. Ten μl samples of the supernatant were diluted with 70 μl of borate buffer to which 20 μl aliquots of 6-aminoquinol-N-hydroxysuccinimidyl carbamate are added to form fluorescent derivatives. After heating the mixture for 10 min at 37°C, 10 μL of derivatized sample was injected into the HPLC system, consisting of a Waters 712 Autosampler, two 510 HPLC pumps, column heater (37°C) and the fluorescence detector. Separation of amino acids was accomplished using a Waters amino acid column and supplied buffers (A – 19% sodium acetate, 7% phosphoric acid, 2% triethylamine, 72% water; B – 60% acetonitrile) following an empirically designed gradient profile. HPLC control and data acquisition were managed by Millennium 32 software. Possible genotype differences were determined using Student's t-tests for each region and sex.

Western blotting

Detection of midbrain SERT protein by western blot was performed as previously described [104] with minor revisions. Briefly, freshly dissected midbrain samples from male and female mice were homogenized in 50 mM Tris pH 7.4 and then centrifuged at 15,000*xg* for 20 min. The resulting pellets were resuspended in RIPA buffer (50 mM Tris-HCl, pH 8.0, 150 mM NaCl, 1% NP-40, 0.5% sodium deoxycholate and 0.1% sodium dodecyl sulfate (SDS); Sigma-Aldrich, St Louis, MO) containing a protease inhibitor cocktail (Sigma-Aldrich, St Louis, MO, USA). Homogenates were nutated for 1 hr at 4°C and the resulting protein lysates were cleared of any insoluble material by centrifugation for 20 min at 15,000*xg* at 4°C. Protein concentration of the resulting supernatants was determined by the bicinchoninic acid (BCA) assay (Thermo Fisher Scientific, Waltham, MA). 2X Laemmli loading buffer (Bio-Rad Laboratories, Hercules, CA) was added to 50 ug of protein and incubated at room temperature for 12 min. Proteins were separated on a NuPAGE 10% Bis-Tris protein gel (Invitrogen, Carlsbad, CA) and then transferred to Immobilon-FL PVDF membrane (MilliporeSigma, Burlington, MA). Membranes were blocked for 1 hr at room temp in 5% non-fat milk in Tris-buffered saline, 0.1% Tween 20 (TBST). Primary SERT antibody (1:1000 dilution, Guinea pig anti-5HTT, Cat # HTT-GP-

Af1400, RRID:AB2571777 Frontier Institute, Japan)[99] was incubated overnight at 4°C with constant agitation. The next day, membranes were subjected to four 5 min washes in TBST and then probed with IRDye 800RD donkey anti-guinea pig secondary antibody (LI-COR Biosciences, Lincoln, NE). Immunoreactivity was detected using the Odyssey Fc (LI-COR Biosciences, Lincoln, NE) followed by densitometry analysis of protein levels normalized to β-actin using ImageJ.

Synaptosomal [^{3}H]5-HT uptake

Midbrain SERT activity was assessed using midbrain synaptosomes. Male and female mice were sacrificed by rapid decapitation followed by dissection of the midbrain on ice. Samples were immediately homogenized in 3 mL of ice cold 0.32 M sucrose. After a 10 min, 4°C centrifugation at 800*xg*, supernatants were transferred to fresh tubes followed by centrifugation at 15,000 *xg* at 4°C for 20 min. Synaptosomal pellets were resuspended in Krebs-Ringers-HEPES (KRH) assay buffer (130 mM NaCl, 1.3 mM KCl, 2.2 mM $CaCl_2$, 1.2 mM $MgSO_4$, 1.2 mM KH_2PO_4, 10 mM HEPES, 10 mM glucose, 100 μM pargyline, 100 μM ascorbic acid, pH 7.4). After assessing protein concentrations using the BCA method (ThermoFisher, Waltham, MA), 50 μg synaptosomal protein per tube were incubated for 10 min at 37°C with or without paroxetine. Uptake was initiated by adding 1, 5, 10, 50, 100, and 500 nM radiolabeled ^{3}H5-HT (Perkin Elmer, Waltham, MA) with substitution of 90% of the 100 and 500 nM concentrations with unlabeled 5-HT at 37°C for 10 min. Uptake was terminated by rapid washing with ice-cold PBS onto Whatman filters (soaked in 0.3% polyethyleneimine) using a Brandel Cell Harvester (Brandel, Gaithersburg, MD USA). Captured [^{3}H]5-HT was eluted in scintillation liquid (Ecoscint H, National Diagnositics, Charlotte, NC, USA) overnight and quantified using a Wallac scintillation counter. Specific uptake was calculated by subtracting the counts obtained from samples incubated in parallel with 10 μM paroxetine from total counts without paroxetine. Michaelis-Menten curve fit in Prism 7.0 was used to calculate K_M and V_{max} values. Data were analyzed using a one-way ANOVA to determine statistical significance across genotypes.

Behavioral assessment of SERT Ala276 mice

Open Field: In all assays where possible, behavioral assays were performed blind to genotype. Locomotor activity in the open field was measured using 27 x 27 x 20.5 chambers (Med Associates, St. Albans, VT) placed within light- and air-controlled sound-attenuating boxes (64 x 45 x 42 cm). Locomotion was detected by interruption of infrared beams by the body of the mouse (16 photocells in each horizontal axis located 1 cm above the activity chamber floor, as well as 16 photocells elevated 4 cm above the chamber floor to detect rearing and jumping behaviors). Data were collected and analyzed by Med Associates Activity Monitor software. To determine statistical significance across genotypes, the data for each sex were analyzed using a one-way ANOVA.

Elevated Zero Maze: To obtain an index of anxiety, mice were placed in the open zone of a zero maze (Stoelting, Wood Dale, IL). Maze arms were approximately 5 cm wide, with a 0.5 cm lip in the open zones to prevent the mouse from falling. The closed arms of the maze were 20-30 cm tall. The maze was elevated approximately 60 cm from the floor. The maze was cleaned before and after each run with an10% ethanol solution. For the test,

animals were permitted to explore freely while being videotaped from above. At the end of the trial, mice were removed from the maze and returned to the home cage. AnyMaze was used to detect and analyze the mouse position during the 5 min trial. Statistically significant differences across genotypes were determined for each sex using a one-way ANOVA.

Forced Swim Test (FST): To assess stress coping behavior, mice were placed in a large beaker, filled with 25-27° C water such that they cannot escape from the beaker and cannot touch the bottom. On each of two consecutive days, a mouse is placed in the beaker for 5-15 min. Latency to float, and amount of time spent struggling are measured. The experimenter monitors the mouse during the task, either by being within the same room, or in an adjacent room with a live video feed. If there is any indication that the mouse was struggling to keep its mouth above water or was in danger of drowning, it was removed from the beaker immediately and excluded from the study. At the completion of the test, the animal was removed from the beaker, towel dried, and recovered for 10-20 min in a warm cage (~35-37°C) sitting on a heating pad. Possible genotype differences were determined for each sex using one-way ANOVA.

Tail Suspension Test: The tail of a mouse is taped to a vertical aluminum bar connected to a strain gauge inside a commercial tail suspension test chamber (Med Associates, Fairfax, VT). Mice were suspended directly vertically to minimize chances of injury and to decrease the propensity for mice to climb their tail during the test. Mice were monitored for a total of 6 minutes to measures time spent struggling. Experimenters were blind to genotype during the test. To determine statistical significance across genotypes, the data for each sex were analyzed using a one-way ANOVA.

Tube Test: The tube test was used to assess social avoidance and conducted as previously described [103]. For two-day consecutive days prior to the testing day, mice were introduced and allowed to enter and exit the tube apparatus, a 30 cm long, 3.5 cm-diameter clear acrylic tube with small, acrylic funnels attached to each end in order to aid in entry into the tube. On testing day, pairings were run in both directions as previously described to avoid positional bias and were paired off against all counterparts present in opposing home cage [86]. For each testing bout, randomized mice from the same sex and age cohorts but separate and distinct home cages were placed at the opposite ends of the tube and released. Each subject was declared a “winner” when their respective opponent backed out of the tube. If neither animal backed out of the tube after a time period of 2 min, a draw was declared. Draws were excluded from analysis. All wins and losses were included in analysis of data. Assessment of genotype differences were compared to an expected 50:50 distribution using χ^2 test for each sex.

Marble Burying: To obtain a measure of repetitive behavior, mice were placed in individual cages containing ~5 cm of beta chip sawdust bedding or similar (including Harlan, diamond soft bedding) for 15 min to acclimate to the test conditions. After 15 min each mouse was briefly removed from its cage, the bedding was smoothed and slightly compacted, and twenty-five marbles (~1.5 cm) were placed in the cage in 5 rows. The mice were returned to the cage and allowed 20-60 min (most typically 30 min) to investigate the

marbles. At the end of the study, the mice were returned to their home cages and the number of marbles buried at least two-thirds of the way in the bedding was recorded. To determine statistical significance across genotypes, the data were analyzed using a one-way ANOVA for each sex.

Graphical and statistical analyses

GraphPad Prism version 9.0 (GraphPad Software, San Diego, CA, USA) was used to perform all statistical analyses and graph results. Post hoc Tukey's or Dunn's multiple comparison tests were performed following one-, two-way ANOVA or Kruskal-Wallis test where applicable. In all tests, $P < 0.05$ was considered statistically significant.

III. Results

Potential orientations of SERT Thr276, pThr276, and Ala276

To determine and depict the possible structural consequences of phosphorylating hSERT Thr276 to yield hSERT pThr276, as well as Ala substitution to generate the non-phosphorylatable substitution hSERT Ala276, we modeled these changes computationally as described in Methods. Thr276 is located in helix TM5 and is part of the internal packing of that region when SERT is in outwards, in agreement with the low SASA value of T276 in that conformation (SASA 20%). For hSERT in the inward facing conformation, the secondary structure and accessibility of Thr276 changes drastically. Here, the last helical turn of TM4 and the first turn of TM5 (which contains Thr276) unwind (Figure 1a). As a consequence, Thr276 is no longer located within an alpha helix, nor does it take part in the internal packing of the protein, becoming exposed to the solvent (SASA 50%). In fact, Thr276 is clearly visible in the structure and completely exposed to the solvent, which it is also expected to be case when phosphorylated (Figure 1b, c). The extremely different SASA values of Thr276 in outwards and inwards conformations supports the idea that Thr276 is only accessible for phosphorylation by PKG or other kinases activated by PKG phosphorylation when hSERT is in an inward-facing conformation. This accessibility might also be affected by the binding of the different protein partners, which could alter the conformation of this region. Nevertheless, a mechanism that implies the induce-fit motion of Thr276 neighboring regions would probably require an additional energy cost and, therefore, be less likely than one in which just conformational selection is assumed. The Thr276Ala substitution introduces a helical former in a region that changes secondary structure upon conformational change. Since Thr276 is part of a helix when the transporter is in an outward-facing conformation, the introduction of an alanine at that position is predicted to have only a minor impact, if any, on the helicity and helical packing in that region. In contrast, the substitution may induce changes when the transporter is in an inward-facing conformation where part of helices TM 4 and 5 belong to a loop. The introduction of a helical promoting residue in the new loop might favor a more helical configuration in that region which could affect the local packing. However, published *in vitro* data [65,100], and our findings with the Thr276Ala substitution in mouse SERT, assessed *ex vivo* (see below), indicate that this change does not appreciably impact SERT activity.

Generation and initial characterization of the SERT Thr276Ala knock-in mouse

In order to study the *in vivo* impact of SERT phosphorylation at Thr276, we used a CRISPR/Cas9 approach to mutate mouse *Slc6a4* genomic sequence that encodes the Thr residue to Ala, making this site incapable of being phosphorylated and matching the substitution used for this purpose in transfected cell studies [65,67,100] (Figure 2a). One male founder mouse was identified via Sanger Sequencing (Figure 2b) and was used to generate heterozygous (Het) mice that were then extensively backcrossed to WT C57Bl/6J mice in an effort to eliminate off-target mutations. From 63 separate Het breeding pairs across two institutions (Vanderbilt University and Florida Atlantic University), we obtained 861 pups in total which were weaned and genotyped at 3 weeks of age. A significant deviation from the Hardy-Weinberg equilibrium was shown ($P = 0.019$, χ^2 tests). Although we observed a trend toward reduction of homozygous Ala276 males ($P = 0.078$), this effect was mainly driven by a significant decrease of homozygous Ala276 females ($P = 0.015$) (Figure 2c). No significant differences in males and females were observed comparing the weights between genotypes at any point from 4 to 10 weeks of age (two-way RMANOVA; male $p<0.74$: female $P<0.65$) (Figure 2d).

Lack of genotype effects in gross physical and sensorimotor abnormalities for the Ala276 to Thr276 substitution

An extensive Irwin screen of SERT Ala276 mice and their littermates revealed no gross abnormalities. Assessment of the general physical factors such as the presence of whiskers, appearance of fur and general fur condition revealed no significant difference. Next, we observed behavior in a novel environment and also noticed no differences between genotypes in categories such as body position, gait, and tail elevation, among others. Reflexes and motor functions to simple stimuli such as touch were also found to be comparable between WT and SERT Ala276 mice. Finally, mice were subject to supine restraint, where no significant differences between genotypes in behaviors such as provoked biting were observed (Table 1).

SERT mRNA, protein levels, and uptake kinetics are unaltered in SERT Ala276 mice

To determine whether the SERT Ala276 impacts expression of SERT mRNA or protein levels, we performed qPCR and western blot analyses, respectively, using tissue extracts from adult males of each genotype. In both midbrain and hippocampus extracts, no significant genotype effect on mRNA expression was observed in males and females (one-way ANOVA; midbrain males $P = 0.21$; midbrain females $P = 0.39$; hippocampus males $P = 0.66$; hippocampus females $P = 0.62$) (Figure 3a and b). A similar lack of genotype effect was obtained in western blot analyses of midbrain protein and quantified SERT protein expression (Figure 3c). Finally, we evaluated midbrain synaptosomal 5-HT uptake kinetics as a function of genotype. In agreement with our qPCR and western analyses and with studies comparing hSERT Thr276 vs hSERT Ala56 transfected cells, we also observed no difference *ex vivo* in SERT function [65] either in 5-HT K_M or transport V_{max} (Figure 3d).

Lack of effect of SERT Ala276 substitution on neurochemical measures

Next, we sought to determine whether the SERT Ala276 substitution had any effect on levels of tissue neurotransmitter content, particularly 5-HT levels or the 5-HT metabolite 5-HIAA.

We used HPLC to obtain these measures from homozygous WT and SERT Ala276 KI mice (males and females) using extracts of midbrain, hippocampus (Table 2a), cortex, and cerebellum (Table 2b). For no neurotransmitters (5-HT, DA, NE, GABA, glutamate) or metabolite (5-HIAA, DOPAC, HVA) were genotype differences detected (within region Student's t-tests, $P > .05$, n=4-7)).

Lack of effect of SERT Ala276 substitution on activity in the open field locomotor activity and in elevated zero maze

Since both 5-HT and SERT have been extensively studied for their role in depression and anxiety-linked behaviors, we sought to assess if expression of SERT Ala276 in measures commonly used to explore these traits in rodents. To assess anxiety-like behavior, we measured both the time spent in the periphery of an open field arena and time spent in the open arms of the elevated zero maze. Homozygous SERT Ala276 mice displayed no difference in total distance traveled in the open field in either male or female mice ($P > 0.05$, one-way ANOVA followed by Tukey's multiple comparison test) (data not shown), nor does it affect the time spent in the outer edges of the open field area (Figure 4a). In the elevated zero maze test, all mice, regardless of sex or genotype, spent a similar percent of time in the open arms (Figure 4b).

Lack of effect of SERT Ala276 substitution on behavior in the tail suspension and forced swim test

In order to assess stress coping or despair-like behavior, we measured the time immobile in the tail suspension test (TST) and the forced swim test (FST), tests sensitive to SERT-targeted drugs (e.g. SSRIs). For both male and females, all mice displaced similar times spent immobile in the force swim test (Figure 4c). To avoid any forced swim-induced stress that may carry over to the TST, a separate cohort of mice was used for the latter test. Due to allocation of animals to other studies, only male WT and SERT Ala276 KI mice were assessed. Male SERT Ala276 mice showed no difference in the time spent immobile compared to their WT littermates in the TST (Figure 4d).

Sex-dependent impact of SERT Ala276 in test of social interactions and repetitive behavior

Although no behavioral effects were noted in mice with SERT Ala276 alleles, consistent with the lack of functional effects observed in past work *in vitro* and our own biochemical studies, we did observe changes in two assays, and these findings demonstrated conspicuous sex-effects. In the tube test of social dominance, we studied only homozygous genotypes due to animal limitations. Here, we found male SERT Ala276, but not females, to win significantly fewer bouts than WT littermates (Figure 5a). Further, female SERT Ala276 heterozygous and homozygous mice displayed significantly diminished numbers of marbles buried (Figure 5b), whereas males of these genotypes buried similar marbles during the 20-minute session as their WT littermates. The lack of effect in males should be considered preliminary though due to the high variability detected in these animals.

IV. Discussion

Our prior review of the Thr276 variant highlighted aspects of the site's phosphorylation leading to conformational bias and functional changes arising from phosphorylation. To better understand and visualize the accessibility of this residue, we pursued a modeling effort based on the availability of structures of hSERT in different conformations [97,105]. We took advantage not only of the structural data available but also of the template-based molecular modelling technique to inspect potential effects of phosphorylation at Thr276 in hSERT, for which evidence has been provided via biochemical studies [65,67] and direct probing with a pThr276 antibody [100]. The resolution of the models obtained using template-based approaches depend mainly on the percentage of sequence identity between the template and the query used [59]. The accuracy of the outwards hSERT model obtained in this work is extremely high and comparable to that of the template structure as indicated by the ~100% sequence identity. It is worth noting that this is the case because the modelling procedure was only used to reverse several mutations present in the X-ray structure.
We focused on determining whether phosphorylation of hSERT Thr276 is likely to be conformation-dependent and the possible effects that this modification would have on local packing. For this purpose, we compared the location and solvent accessibility of Thr276 in the transmembrane domain of hSERT in the outward-facing models and inward-facing structure 6dzz [105]. The structural analysis indicates that for the outward conformation, Thr276 is located in a helix at a site that is likely not exposed to the cytoplasm (SASA value 20%) where it takes part in the local interacting network that stabilizes the fold in that region. This interacting network is not present in the inward facing conformation due to a local unwinding of TM4 and TM5 which positions Thr276 in a loop only present in this conformation. The secondary structural change of Thr276 between conformations, from helical in outwards to coil in inwards, affects the solvent accessibility of the residue, which goes from being occluded to being solvent-exposed (SASA of 50%). Our modeling thus suggests that the phosphorylation of Thr276 likely occurs in an inward-facing conformation as the accessibility of the residue would be required for the cytoplasmic kinase to target the residue.

Secondly, the introduction of a negatively charged and bulky phosphate at position 276 would likely, without other accommodations, obstruct the reformation of the local helical structure in TM4 and TM5 observed in the outward-facing conformation, consistent with phosphorylation increasing the energy barrier return of the unloaded carrier to an outwards-facing state. However, as noted, prior data [65,67] show quite the opposite, with phosphorylation of Thr276-hSERT increasing transport rate of SERT. Thus, other modifications or local conformational adjustments must arise that can overcome this barrier and that will need to be elucidated experimentally. Possibly changes in the electrostatic potential as a result of phosphorylation at Thr276 might favor K^+ or H^+ binding, believed to reduce a major energy barrier that allows the transporter to return to the outward state [2]. As we do not have a K^+ bound structure, whether phosphorylation with its added negative charge facilitates the binding of the cation to initiate cycle translocation cannot be presently discerned but is an important aspect to be investigated structurally and biochemically in the future. Finally, phosphorylation of this juxta-membrane residue could affect the trafficking

of SERT from cytoplasmic vesicles to the membrane, which is similarly speculative but presumably could involve changes in protein-protein interactions or arise by prevention of post-translational modifications that drive basal endocytic rates.

Ultimately, the functional significance of studies examining SERT Thr276 phosphorylation through *in vitro* or modeling studies requires movement to an *in vivo* model where phosphorylation is either precluded or mimicked genetically. Here we describe the generation of the former model, namely a SERT Ala276 mouse line, on a C57Bl/6J mouse background. We show these mice to be viable and to grow normally. However, we saw a deviation from a Mendelian distribution with a reduction in homozygous male and female offspring. This raises questions as to a requirement for SERT phosphorylation in relation to embryonic growth or neonatal survival of mice. Placental serotonin is important during fetal brain development and alterations in placental 5-HT synthesis negatively affects the structure and function of the brain [79]. Even though our mice were bred using heterozygous pairs, a recent study provided evidence that pups from dams homozygous for the SERT Ala56 allele show alterations in 5-HT levels in the developing forebrain and the organization of thalamocortical projections [102]. However, no significant changes were found in heterozygous dams. We did obtain evidence that heterozygous females show a difference in marble burying suggesting that the Ala276 allele, and by inference a need for SERT phosphorylation, can have dominant effects in some contexts.

Use of an extensive Irwin screen revealed no differences between genotypes in general physical appearance, motor abilities, reflexes or sensory function in SERT Ala276 animals. We also found no changes in SERT mRNA and protein levels. With the successful baseline characterization of this mouse line, our interests immediately turned to analysis of 5-HT-linked behaviors. Though kinetic analyses revealed no differences in 5-HT uptake in mice with the mutant allele compared to WT mice, we hypothesized that behavioral changes may still result from loss of dynamic SERT regulation. In the open field, tail suspension, forced swim and elevated zero maze tests, however, SERT Ala276 displayed comparable behaviors to WT littermates. Future studies will aim to determine if these assays can reveal genotype differences when SSRIs, psychoactive agents that impose conformational bias in SERT such as ibogaine [64,100] and SERT targeting psychostimulants. This idea seems particularly relevant given evidence that substrates can impact phosphorylation of hSERT following protein kinase C activation [37]. Interestingly, SERT Ala276 mice demonstrated sex-dependent changes in two behavioral measures. Female but not male SERT Ala276 mice exhibited a significant reduction in marble burying relative to littermates expressing wildtype SERT. Alterations in marble burying have been observed in monoamine oxidase A deficient mice, effects that can be reversed by SSRIs, indicating that the phenotype is sensitive to genetic perturbations in 5-HT homeostasis in a manner than can engage SERT-dependent processes [90]. Consistent with this idea, SERT KO mice demonstrated a reduction in marble burying [60], suggesting that the phenotype is worth further evaluation in relation to task-dependent assays. Additionally, male, but not female, SERT Ala276 mice demonstrate altered social behavior as assessed in the tube test, mirroring alterations previously observed in SERT Ala56 mice developed to model genetically-determined serotonergic contributions to ASD [86]. The similarity of phenotypes between SERT Ala276

and SERT Ala56 might rely on interactions between the structural domains harboring these residues.

V. Future Directions

Amino acid Thr276 of SERT has been identified as a critical phosphorylation site for PKG dependent regulation of the transporter [65]. However, the role or requirement for phosphorylation at this site *in vivo* has been unexplored. The generation of the SERT Ala276 knock-in mouse model provides a platform to address the function of SERT Thr276 phosphorylation in respect to transporter function and downstream, circuit level effects *in vivo* [65,100]. Our future studies will seek to confirm loss of PKG-induced phosphorylation of SERT in the Ala276 mice as well as to determine whether p38α MAPK involvement in PKG-mediated SERT regulation occurs through this residue. Several *in vitro* studies have shown that PKG activation results in both a trafficking-dependent and -independent change that elevates rates of 5-HT uptake, with the latter effect being mediated by p38α MAPK activation [50,82]. It is well known that proinflammatory cytokines and stress activate p38 MAPK [40] and we have shown that inflammatory stimuli, such as IL-1β and the bacterial mimetic lipopolysaccharide (LPS) increase 5-HT transport in a p38 MAPK dependent manner [78,92]. In mice, intraperitoneal injection of LPS also lead to depression-like behaviors such as increased immobility in TST and FST [78], with conditional elimination of p38α MAPK in serotonergic neurons rescuing these phenotypes [92]. It would therefore be interesting to also investigate whether phosphorylation of Thr276 is required for SERT regulation after immune activation.

SERT is the primary target of a number of critical therapeutics and drugs of abuse including SSRIs and psychostimulants such as 3,4-methylenedioxymethamphetamine (MDMA) whose actions may be altered in SERT Thr276 mice. A recent study reported that the prosocial effect of MDMA is mediated by SERT and can be mimicked by injections of the selective 5-HT releasing drug fenfluramine [106]. Since transporter conformation alters fenfluramine-induced 5-HT efflux [107] changes in social behavior should be investigated further, with and without MDMA-like agents, in order to evaluate a role for SERT Thr276 phosphorylation *in vivo*. We recently demonstrated that the hyperactive and hyperphosphorylated SERT variant Ala56 biases the transporter towards an outward-open conformation [107]. One might consider that, the Ala276 variant might bias SERT towards an inward-open state since the transporter loses PKG-induced phospho-regulation. However, as mentioned above, Thr276 lies in the cytoplasmic end of the TM5 helix which changes its conformation when the transporter cycles from the outward- to the inward-open state. This helix partially unwinds and extends the region containing Thr276 into the cytoplasm which potentially makes the site accessible to kinases [95]. Moreover, a biased inward state would be more consistent with loss, not gain of activity. We suggest that the phosphorylation at Thr276 may produce conformations that facilitate return of the unloaded carrier, though this cannot be inferred from present models. Additionally, the amino and carboxy termini are believed to exist in closer proximity when the transporter resides in the outward-open state [89,107], and this several potential phosphorylation sites in the terminal domains for p38 MAPK and PKC [91] might become inaccessible to mediate changes in SERT activity in response to transporter phosphorylation in SERT Ala276.

The kinase(s) responsible for SERT phospho-regulation at Thr276 have also yet to be determined. Several studies provided evidence that PKG does not directly phosphorylate Thr276 [91,100]. There is, however, evidence that hSERT Ser277 represents a phosphorylation site for PKC [91]. For NET, the corresponding Thr258 and S259 sites are sites of PKC-mediated phosphorylation of which Ser259 is phosphorylated before Thr258 [51]. Therefore, PKG might act via another kinase to phosphorylate Thr276 which then precludes exposure of Ser277 to PKC leading to reduced endocytosis. Such a model could explain the role of Thr276 in transporter surface trafficking reported following PKG activation. In summary, we believe that the Ala276 mouse model can allow us to further dissect the requirements for kinase-dependent SERT modulation in 5-HT signaling, circuit level plasticities and behavior. Ultimately, we hope that studies of this novel mouse model will contribute to the understanding of the physiological significance of SERT regulation through kinases and further support the development of new genetical or pharmacological methods to better treat neuropsychiatric disorders that feature perturbed serotonergic function or might benefit from a more nuanced manipulation of SERT compared to a full blockade of the transporter achieved through the use of SSRIs.

Acknowledgement:

All behavioral testing was conducted in the Vanderbilt Neurobehavioral Core Facility whereas HPLC-based neurotransmitter analyses were conducted in the Neurochemistry Core, both operated by the Vanderbilt Brain Institute, and the Vanderbilt Kennedy Center, supported by NIH Award U54HD083211. CRISPR/Cas9 mediated modification of sequences encoding the SERT Thr276 residue and generation of SERT Ala276 mice were carried out through the Vanderbilt Genome Editing Resource operated by the Vanderbilt Center for Stem Cell Biology which is supported by NIH award CA68485 to the Vanderbilt Cancer Center Support Grant and DK020593 to the Vanderbilt Diabetes Research and Training Center. We gratefully acknowledge the support of Matthew Gross for his outstanding laboratory support. Finally, we gratefully acknowledge the pioneering work of Baruch Kanner whose decades long efforts to elucidate structural and functional properties of neurotransmitter transporters cannot be understated, in recognition of which we dedicate this article

Funding:

The project was supported by NIH award MH094527 to RDB and MH112731 to SR. CF-F was supported by the National Institutes of Health Intramural Research Program of the NIDCD via award DC000048 to Thomas B. Friedman and to DC000060 to Isabelle Roux.

References

1. Irwin S (1968) Comprehensive observational assessment: Ia. A systematic, quantitative procedure for assessing the behavioral and physiologic state of the mouse. Psychopharmacologia 13 (3):222–257. doi:10.1007/bf00401402 [PubMed: 5679627]
2. Rudnick G, Nelson PJ (1978) Platelet 5-hydroxytryptamine transport, an electroneutral mechanism coupled to potassium. Biochemistry 17 (22):4739–4742. doi:10.1021/bi00615a021 [PubMed: 728383]
3. Kanner BI, Schuldiner S (1987) Mechanism of transport and storage of neurotransmitter. Critical Reviews in Biochemistry and Molecular Biology 22 (1):1–38. doi:10.3109/10409238709082546
4. Fuller RW, Wong DT (1990) Serotonin Uptake and Serotonin Uptake Inhibition. Annals of the New York Academy of Sciences 600 (1):68–80. doi:10.1111/j.1749-6632.1990.tb16873.x [PubMed: 2252338]
5. Kemp BE, Pearson RB (1990) Protein kinase recognition sequence motifs. Elsevier Science Publishers Ltd 15 (September):342–346. doi:10.1016/0968-0004(90)90073-k

6. Bastani B, Arora RC, Meltzer HY (1991) Serotonin uptake and imipramine binding in the blood platelets of obsessive-compulsive disorder patients. Biological Psychiatry 30 (2):131–139. doi:10.1016/0006-3223(91)90166-j [PubMed: 1655071]
7. Blakely RD, Berson HE, Fremeau RT Jr., Caron MG, Peek MM, Princet HK, Bradleyt CC (1991) Cloning and expression of a functional SERT from rat brain. Nature 354:66–70 [PubMed: 1944572]
8. Hoffman BJ, Mezey E, Brownstein MJ (1991) Cloning of a serotonin transporter affected by antidepressants. Science 254 (5031):579. doi:10.1126/science.1948036 [PubMed: 1948036]
9. Kennelly PJ, Krebs EG (1991) Consensus sequences as substrate specificity determinants for protein kinases and protein phosphatases. Journal of Biological Chemistry 266 (24):15555–15558 [PubMed: 1651913]
10. Nicholls A, Sharp KA, Honig B (1991) Protein folding and association: Insights from the interfacial and thermodynamic properties of hydrocarbons. Proteins: Structure, Function, and Bioinformatics 11 (4):281–296. doi:10.1002/prot.340110407
11. Pacholczyk T, Blakely RD, Amara SG (1991) Expression cloning of a cocaine-and antidepressant-sensitive human noradrenaline transporter. Nature 350 (6316):350–354. doi:10.1038/350350a0 [PubMed: 2008212]
12. Clark JA, Amara SG (1993) Amino acid neurotransmitter transporters: structure, function, and molecular diversity. Bioessays 15 (5):323–332. doi:10.1002/bies.950150506 [PubMed: 8102052]
13. Laskowski RA, MacArthur MW, Moss DS, Thornton JM (1993) PROCHECK: a program to check the stereochemical quality of protein structures. Journal of Applied Crystallography 26 (2):283–291. doi:10.1107/S0021889892009944
14. Ramamoorthy S, Bauman AL, Moore KR, Han H, Yang-Feng T, Chang AS, Ganapathy V, Blakely RD (1993) Antidepressant- and cocaine-sensitive human serotonin transporter: molecular cloning, expression, and chromosomal localization. Proc Natl Acad Sci U S A 90 (6):2542–2546. doi:10.1073/pnas.90.6.2542 [PubMed: 7681602]
15. Rudnick G, Clark J (1993) From synapse to vesicle: the reuptake and storage of biogenic amine neurotransmitters. Biochim Biophys Acta 1144 (3):249–263. doi:10.1016/0005-2728(93)90109-s [PubMed: 8104483]
16. Šali A, Blundell TL (1993) Comparative Protein Modelling by Satisfaction of Spatial Restraints. Journal of Molecular Biology 234 (3):779–815. doi:10.1006/jmbi.1993.1626 [PubMed: 8254673]
17. Jayanthi LD, Ramamoorthy S, Mahesh VB, Leibach FH (1994) Calmodulin-dependent Regulation of the Catalytic Function of the Human Serotonin Transporter in Placental Choriocarcinoma Cells *. J Biol Chem 269 (20):14424–14429 [PubMed: 8182048]
18. Melikian HE, McDonald JK, Gu H, Rudnick G, Moore KR, Blakely RD (1994) Human norepinephrine transporter. Biosynthetic studies using a site-directed polyclonal antibody. Journal of Biological Chemistry 269 (16):12290–12297 [PubMed: 8163533]
19. Miller KJ, Hoffman BJ (1994) Adenosine A3 receptors regulate serotonin transport via nitric oxide and cGMP. J Biol Chem 269 (44):27351–27356 [PubMed: 7525554]
20. Owens MJ, Nemeroff CB (1994) Role of serotonin in the pathophysiology of depression: focus on the serotonin transporter. Clin Chem 40 (2):288–295 [PubMed: 7508830]
21. Tate CG, Blakely RD (1994) The effect of N-linked glycosylation on activity of the Na+- and Cl−-dependent serotonin transporter expressed using recombinant baculovirus in insect cells. J Biol Chem 269 (42):26303–26310 [PubMed: 7523405]
22. Thompson JD, Higgins DG, Gibson TJ (1994) CLUSTAL W: improving the sensitivity of progressive multiple sequence alignment through sequence weighting, position-specific gap penalties and weight matrix choice. Nucleic Acids Res 22 (22):4673–4680. doi:10.1093/nar/22.22.4673 [PubMed: 7984417]
23. Bruss M, Hammermann R, Brimijoin S, Bonisch H (1995) Antipeptide antibodies confirm the topology of the human norepinephrine transporter. vol 270. doi:10.1074/jbc.270.16.9197
24. Montgomery SA (1995) Psychopharmacology: The fourth generation of progress. Raven Press, Ltd., New York
25. Qian Y, Melikian HE, Rye DB, Levey AI, Blakely RD (1995) Identification and characterization of antidepressant-sensitive serotonin transporter proteins using site-specific antibodies. J Neurosci 15 (2):1261–1274. doi:10.1523/jneurosci.15-02-01261.1995 [PubMed: 7869097]

26. Ramamoorthy JD, Ramamoorthy S, Papapetropoulos A, Catravas JD, Leibach FH, Ganapathy V (1995) Cyclic AMP-independent Up-regulation of the Human Serotonin Transporter by Staurosporine in Choriocarcinoma Cells. J. Biol. Chem doi:doi:10.1074/jbc.270.29.17189
27. Chang AS, Chang SM, Starnes DM, Schroeter S, Bauman AL, Blakely RD (1996) Cloning and expression of the mouse serotonin transporter. Brain Res Mol Brain Res 43 (1-2):185–192. doi:10.1016/s0169-328x(96)00172-6 [PubMed: 9037532]
28. Vaughan RA, Kuhar MJ (1996) Dopamine transporter ligand binding domains. Structural and functional properties revealed by limited proteolysis. J Biol Chem 271 (35):21672–21680. doi:10.1074/jbc.271.35.21672 [PubMed: 8702957]
29. Blakely RD, Ramamoorthy S, Qian Y, Schroeter S, Bradley CC (1997) Regulation of Antidepressant-Sensitive Serotonin Transporters. In: Reith MEA (ed) Neurotransmitter Transporters. Humana Press, Totowa, NJ, pp 29–72. doi:10.1007/978-1-59259-470-2_2
30. Chen JG, Sachpatzidis A, Rudnick G (1997) The third transmembrane domain of the serotonin transporter contains residues associated with substrate and cocaine binding. J Biol Chem 272 (45):28321–28327. doi:10.1074/jbc.272.45.28321 [PubMed: 9353288]
31. Qian Y, Galli A, Ramamoorthy S, Risso S, DeFelice LJ, Blakely RD (1997) Protein kinase C activation regulates human serotonin transporters in HEK-293 cells via altered cell surface expression. J Neurosci 17 (1):45–57. doi:10.1523/jneurosci.17-01-00045.1997 [PubMed: 8987735]
32. Tatsumi M, Groshan K, Blakely RD, Richelson E (1997) Pharmacological profile of antidepressants and related compounds at human monoamine transporters.
33. Vaughan RA, Huff RA, Uhl GR, Kuhar MJ (1997) Protein kinase C-mediated phosphorylation and functional regulation of dopamine transporters in striatal synaptosomes. J Biol Chem 272 (24):15541–15546. doi:10.1074/jbc.272.24.15541 [PubMed: 9182590]
34. Chen JG, Liu-Chen S, Rudnick G (1998) Determination of external loop topology in the serotonin transporter by site-directed chemical labeling. J Biol Chem 273 (20):12675–12681. doi:10.1074/jbc.273.20.12675 [PubMed: 9575231]
35. Ferrer JV, Javitch JA (1998) Cocaine alters the accessibility of endogenous cysteines in putative extracellular and intracellular loops of the human dopamine transporter. Proceedings of the National Academy of Sciences 95 (16):9238. doi:10.1073/pnas.95.16.9238
36. Ramamoorthy S, Giovanetti E, Qian Y, Blakely RD (1998) Phosphorylation and regulation of antidepressant-sensitive serotonin transporters. J Biol Chem 273 (4):2458–2466. doi:10.1074/jbc.273.4.2458 [PubMed: 9442097]
37. Ramamoorthy S, Blakely RD (1999) Phosphorylation and sequestration of serotonin transporters differentially modulated by psychostimulants. Science 285 (5428):763–766. doi:10.1126/science.285.5428.763 [PubMed: 10427004]
38. Association AP (2000) Diagnostic and Statistical Manual of Mental Disorders-Text Revision (DSM-IV-TR). 4th editio edn. American Psychiatric Association Press, Washington, DC
39. Blakely RD, Bauman AL (2000) Biogenic amine transporters: regulation in flux. Curr Opin Neurobiol 10 (3):328–336. doi:10.1016/s0959-4388(00)00088-x [PubMed: 10851182]
40. Obata T, Brown GE, Yaffe MB (2000) MAP kinase pathways activated by stress: the p38 MAPK pathway. Crit Care Med 28 (4 Suppl):N67–77. doi:10.1097/00003246-200004001-00008 [PubMed: 10807318]
41. Androutsellis-Theotokis A, Ghassemi F, Rudnick G (2001) A conformationally sensitive residue on the cytoplasmic surface of serotonin transporter. J Biol Chem 276 (49):45933–45938. doi:10.1074/jbc.M107462200 [PubMed: 11592963]
42. Machacek DW, Garraway SM, Shay BL, Hochman S (2001) Serotonin 5-HT(2) receptor activation induces a long-lasting amplification of spinal reflex actions in the rat. J Physiol 537 (Pt 1):201–207. doi:10.1111/j.1469-7793.2001.0201k.x [PubMed: 11711573]
43. Androutsellis-Theotokis A, Rudnick G (2002) Accessibility and conformational coupling in serotonin transporter predicted internal domains. J Neurosci 22 (19):8370–8378 [PubMed: 12351711]

44. Quick MW (2002) Role of syntaxin 1A on serotonin transporter expression in developing thalamocortical neurons. Int J Dev Neurosci 20 (3–5):219–224. doi:10.1016/s0736-5748(02)00021-7 [PubMed: 12175857]
45. Kilic F, Murphy DL, Rudnick G (2003) A human serotonin transporter mutation causes constitutive activation of transport activity. Mol Pharmacol 64 (2):440–446. doi:10.1124/mol.64.2.440 [PubMed: 12869649]
46. Ozaki N, Goldman D, Kaye WH, Plotnicov K, Greenberg BD, Lappalainen J, Rudnick G, Murphy DL (2003) Serotonin transporter missense mutation associated with a complex neuropsychiatric phenotype. Mol Psychiatry 8 (11):933–936. doi:10.1038/sj.mp.4001365 [PubMed: 14593431]
47. Chen NH, Reith ME, Quick MW (2004) Synaptic uptake and beyond: the sodium- and chloride-dependent neurotransmitter transporter family SLC6. Pflugers Arch 447 (5):519–531. doi:10.1007/s00424-003-1064-5 [PubMed: 12719981]
48. Khoshbouei H, Sen N, Guptaroy B, Johnson L, Lund D, Gnegy ME, Galli A, Javitch JA (2004) N-terminal phosphorylation of the dopamine transporter is required for amphetamine-induced efflux. PLoS Biol 2 (3):E78. doi:10.1371/journal.pbio.0020078 [PubMed: 15024426]
49. Murphy DL, Lerner A, Rudnick G, Lesch KP (2004) Serotonin transporter: gene, genetic disorders, and pharmacogenetics. Mol Interv 4 (2):109–123. doi:10.1124/mi.4.2.8 [PubMed: 15087484]
50. Zhu CB, Hewlett WA, Feoktistov I, Biaggioni I, Blakely RD (2004) Adenosine receptor, protein kinase G, and p38 mitogen-activated protein kinase-dependent up-regulation of serotonin transporters involves both transporter trafficking and activation. Mol Pharmacol 65 (6):1462–1474. doi:10.1124/mol.65.6.1462 [PubMed: 15155839]
51. Jayanthi LD, Samuvel DJ, Blakely RD, Ramamoorthy S (2005) Evidence for biphasic effects of protein kinase C on serotonin transporter function, endocytosis, and phosphorylation. Mol Pharmacol 67 (6):2077–2087. doi:10.1124/mol.104.009555 [PubMed: 15774771]
52. Prasad HC, Zhu CB, McCauley JL, Samuvel DJ, Ramamoorthy S, Shelton RC, Hewlett WA, Sutcliffe JS, Blakely RD (2005) Human serotonin transporter variants display altered sensitivity to protein kinase G and p38 mitogen-activated protein kinase. Proc Natl Acad Sci U S A 102 (32):11545–11550. doi:10.1073/pnas.0501432102 [PubMed: 16055563]
53. Samuvel DJ, Jayanthi LD, Bhat NR, Ramamoorthy S (2005) A role for p38 mitogen-activated protein kinase in the regulation of the serotonin transporter: evidence for distinct cellular mechanisms involved in transporter surface expression. J Neurosci 25 (1):29–41. doi:10.1523/JNEUROSCI.3754-04.2005 [PubMed: 15634764]
54. Sutcliffe JS, Delahanty RJ, Prasad HC, McCauley JL, Han Q, Jiang L, Li C, Folstein SE, Blakely RD (2005) Allelic heterogeneity at the serotonin transporter locus (SLC6A4) confers susceptibility to autism and rigid-compulsive behaviors. Am J Hum Genet 77 (2):265–279. doi:10.1086/432648 [PubMed: 15995945]
55. Yamashita A, Singh SK, Kawate T, Jin Y, Gouaux E (2005) Crystal structure of a bacterial homologue of Na+/Cl−-dependent neurotransmitter transporters. Nature 437 (7056):215–223. doi:10.1038/nature03978 [PubMed: 16041361]
56. Zhang YW, Rudnick G (2005) Cysteine-scanning mutagenesis of serotonin transporter intracellular loop 2 suggests an alpha-helical conformation. J Biol Chem 280 (35):30807–30813. doi:10.1074/jbc.M504087200 [PubMed: 15994310]
57. Zhu CB, Carneiro AM, Dostmann WR, Hewlett WA, Blakely RD (2005) p38 MAPK activation elevates serotonin transport activity via a trafficking-independent, protein phosphatase 2A-dependent process. J Biol Chem 280 (16):15649–15658. doi:10.1074/jbc.M410858200 [PubMed: 15728187]
58. Carneiro AMD, Blakely RD (2006) Redistribution of the Platelet Serotonin Transporter *. 281 (34):24769–24780. doi:10.1074/jbc.M603877200
59. Forrest LR, Tang CL, Honig B (2006) On the accuracy of homology modeling and sequence alignment methods applied to membrane proteins. Biophys J 91 (2):508–517. doi:10.1529/biophysj.106.082313 [PubMed: 16648166]
60. Kalueff AV, Gallagher PS, Murphy DL (2006) Are serotonin transporter knockout mice ‘depressed’?: hypoactivity but no anhedonia. NeuroReport 17 (12)

61. Zhang YW, Rudnick G (2006) The cytoplasmic substrate permeation pathway of serotonin transporter. J Biol Chem 281 (47):36213–36220. doi:10.1074/jbc.M605468200 [PubMed: 17008313]
62. Zhu CB, Blakely RD, Hewlett WA (2006) The proinflammatory cytokines interleukin-1beta and tumor necrosis factor-alpha activate serotonin transporters. Neuropsychopharmacology 31 (10):2121–2131. doi:10.1038/sj.npp.1301029 [PubMed: 16452991]
63. Hahn MK, Blakely RD (2007) The functional impact of SLC6 transporter genetic variation. Annu Rev Pharmacol Toxicol 47:401–441. doi:10.1146/annurev.pharmtox.47.120505.105242 [PubMed: 17067279]
64. Jacobs MT, Zhang Y-W, Campbell SD, Rudnick G (2007) Ibogaine, a Noncompetitive Inhibitor of Serotonin Transport, Acts by Stabilizing the Cytoplasm-facing State of the Transporter. Journal of Biological Chemistry 282 (40):29441–29447 [PubMed: 17698848]
65. Ramamoorthy S, Samuvel DJ, Buck ER, Rudnick G, Jayanthi LD (2007) Phosphorylation of threonine residue 276 is required for acute regulation of serotonin transporter by cyclic GMP. J Biol Chem 282 (16):11639–11647. doi:10.1074/jbc.M611353200 [PubMed: 17310063]
66. Sibille E, Su J, Leman S, Le Guisquet AM, Ibarguen-Vargas Y, Joeyen-Waldorf J, Glorioso C, Tseng GC, Pezzone M, Hen R, Belzung C (2007) Lack of serotonin1B receptor expression leads to age-related motor dysfunction, early onset of brain molecular aging and reduced longevity. Mol Psychiatry 12 (11):1042–1056, 1975. doi:10.1038/sj.mp.4001990 [PubMed: 17420766]
67. Zhang YW, Gesmonde J, Ramamoorthy S, Rudnick G (2007) Serotonin transporter phosphorylation by cGMP-dependent protein kinase is altered by a mutation associated with obsessive compulsive disorder. J Neurosci 27 (40):10878–10886. doi:10.1523/JNEUROSCI.0034-07.2007 [PubMed: 17913921]
68. Ciccone MA, Timmons M, Phillips A, Quick MW (2008) Calcium/calmodulin-dependent kinase II regulates the interaction between the serotonin transporter and syntaxin 1A. Neuropharmacology 55 (5):763–770. doi:10.1016/j.neuropharm.2008.06.018 [PubMed: 18602929]
69. Forrest LR, Zhang YW, Jacobs MT, Gesmonde J, Xie L, Honig BH, Rudnick G (2008) Mechanism for alternating access in neurotransmitter transporters. Proc Natl Acad Sci U S A 105 (30):10338–10343. doi:10.1073/pnas.0804659105 [PubMed: 18647834]
70. Schmittgen TD, Livak KJ (2008) Analyzing real-time PCR data by the comparative C(T) method. Nat Protoc 3 (6):1101–1108. doi:10.1038/nprot.2008.73 [PubMed: 18546601]
71. Singh SK, Piscitelli CL, Yamashita A, Gouaux E (2008) A competitive inhibitor traps LeuT in an open-to-out conformation. Science 322 (5908):1655–1661. doi:10.1126/science.1166777 [PubMed: 19074341]
72. Steiner JA, Carneiro AM, Blakely RD (2008) Going with the flow: trafficking-dependent and -independent regulation of serotonin transport. Traffic 9 (9):1393–1402. doi:10.1111/j.1600-0854.2008.00757.x [PubMed: 18445122]
73. Forrest LR, Rudnick G (2009) The rocking bundle: a mechanism for ion-coupled solute flux by symmetrical transporters. Physiology (Bethesda) 24 (1):377–386. doi:10.1152/physiol.00030.2009 [PubMed: 19996368]
74. Prasad HC, Steiner JA, Sutcliffe JS, Blakely RD (2009) Enhanced activity of human serotonin transporter variants associated with autism. Philos Trans R Soc Lond B Biol Sci 364 (1514):163–173. doi:10.1098/rstb.2008.0143 [PubMed: 18957375]
75. Veenstra-Vanderweele J, Jessen TN, Thompson BJ, Carter M, Prasad HC, Steiner JA, Sutcliffe JS, Blakely RD (2009) Modeling rare gene variation to gain insight into the oldest biomarker in autism: construction of the serotonin transporter Gly56Ala knock-in mouse. J Neurodev Disord 1 (2):158–171. doi:10.1007/s11689-009-9020-0 [PubMed: 19960097]
76. Field JR, Henry LK, Blakely RD (2010) Transmembrane domain 6 of the human serotonin transporter contributes to an aqueously accessible binding pocket for serotonin and the psychostimulant 3,4-methylene dioxymethamphetamine. J Biol Chem 285 (15):11270–11280. doi:10.1074/jbc.M109.093658 [PubMed: 20159976]
77. Sucic S, Dallinger S, Zdrazil B, Weissensteiner R, Jorgensen TN, Holy M, Kudlacek O, Seidel S, Cha JH, Gether U, Newman AH, Ecker GF, Freissmuth M, Sitte HH (2010) The N terminus

of monoamine transporters is a lever required for the action of amphetamines. J Biol Chem 285 (14):10924–10938. doi:10.1074/jbc.M109.083154 [PubMed: 20118234]

78. Zhu CB, Lindler KM, Owens AW, Daws LC, Blakely RD, Hewlett WA (2010) Interleukin-1 receptor activation by systemic lipopolysaccharide induces behavioral despair linked to MAPK regulation of CNS serotonin transporters. Neuropsychopharmacology 35 (13):2510–2520. doi:10.1038/npp.2010.116 [PubMed: 20827273]
79. Bonnin A, Goeden N, Chen K, Wilson ML, King J, Shih JC, Blakely RD, Deneris ES, Levitt P (2011) A transient placental source of serotonin for the fetal forebrain. Nature 472 (7343):347–350. doi:10.1038/nature09972 [PubMed: 21512572]
80. Horvath GA, Selby K, Poskitt K, Hyland K, Waters PJ, Coulter-Mackie M, Stockler-Ipsiroglu SG (2011) Hemiplegic migraine, seizures, progressive spastic paraparesis, mood disorder, and coma in siblings with low systemic serotonin. Cephalalgia 31 (15):1580–1586. doi:10.1177/0333102411420584 [PubMed: 22013141]
81. Zhao Y, Terry DS, Shi L, Quick M, Weinstein H, Blanchard SC, Javitch JA (2011) Substrate-modulated gating dynamics in a Na+-coupled neurotransmitter transporter homologue. Nature 474 (7349):109–113. doi:10.1038/nature09971 [PubMed: 21516104]
82. Chang JC, Tomlinson ID, Warnement MR, Ustione A, Carneiro AM, Piston DW, Blakely RD, Rosenthal SJ (2012) Single molecule analysis of serotonin transporter regulation using antagonist-conjugated quantum dots reveals restricted, p38 MAPK-dependent mobilization underlying uptake activation. J Neurosci 32 (26):8919–8929. doi:10.1523/JNEUROSCI.0048-12.2012 [PubMed: 22745492]
83. Enjin A, Leao KE, Mikulovic S, Le Merre P, Tourtellotte WG, Kullander K (2012) Sensorimotor function is modulated by the serotonin receptor 1d, a novel marker for gamma motor neurons. Mol Cell Neurosci 49 (3):322–332. doi:10.1016/j.mcn.2012.01.003 [PubMed: 22273508]
84. Foster JD, Yang JW, Moritz AE, Challasivakanaka S, Smith MA, Holy M, Wilebski K, Sitte HH, Vaughan RA (2012) Dopamine transporter phosphorylation site threonine 53 regulates substrate reuptake and amphetamine-stimulated efflux. J Biol Chem 287 (35):29702–29712. doi:10.1074/jbc.M112.367706 [PubMed: 22722938]
85. Krishnamurthy H, Gouaux E (2012) X-ray structures of LeuT in substrate-free outward-open and apo inward-open states. Nature 481 (7382):469–474. doi:10.1038/nature10737 [PubMed: 22230955]
86. Veenstra-VanderWeele J, Muller CL, Iwamoto H, Sauer JE, Owens WA, Shah CR, Cohen J, Mannangatti P, Jessen T, Thompson BJ, Ye R, Kerr TM, Carneiro AM, Crawley JN, Sanders-Bush E, McMahon DG, Ramamoorthy S, Daws LC, Sutcliffe JS, Blakely RD (2012) Autism gene variant causes hyperserotonemia, serotonin receptor hypersensitivity, social impairment and repetitive behavior. Proc Natl Acad Sci U S A 109 (14):5469–5474. doi:10.1073/pnas.1112345109 [PubMed: 22431635]
87. Wong A, Zhang YW, Jeschke GR, Turk BE, Rudnick G (2012) Cyclic GMP-dependent stimulation of serotonin transport does not involve direct transporter phosphorylation by cGMP-dependent protein kinase. J Biol Chem 287 (43):36051–36058. doi:10.1074/jbc.M112.394726 [PubMed: 22942288]
88. Penmatsa A, Wang KH, Gouaux E (2013) X-ray structure of dopamine transporter elucidates antidepressant mechanism. Nature 503 (7474):85–90. doi:10.1038/nature12533 [PubMed: 24037379]
89. Fenollar-Ferrer C, Stockner T, Schwarz TC, Pal A, Gotovina J, Hofmaier T, Jayaraman K, Adhikary S, Kudlacek O, Mehdipour AR, Tavoulari S, Rudnick G, Singh SK, Konrat R, Sitte HH, Forrest LR (2014) Structure and regulatory interactions of the cytoplasmic terminal domains of serotonin transporter. Biochemistry 53 (33):5444–5460. doi:10.1021/bi500637f [PubMed: 25093911]
90. Godar SC, Bortolato M, Castelli MP, Casti A, Casu A, Chen K, Ennas MG, Tambaro S, Shih JC (2014) The aggression and behavioral abnormalities associated with monoamine oxidase A deficiency are rescued by acute inhibition of serotonin reuptake. J Psychiatr Res 56:1–9. doi:10.1016/j.jpsychires.2014.04.014 [PubMed: 24882701]

91. Sørensen L, Strømgaard K, Kristensen AS (2014) Characterization of intracellular regions in the human serotonin transporter for phosphorylation sites. ACS Chem Biol 9 (4):935–944. doi:10.1021/cb4007198 [PubMed: 24450286]
92. Baganz NL, Lindler KM, Zhu CB, Smith JT, Robson MJ, Iwamoto H, Deneris ES, Hewlett WA, Blakely RD (2015) A requirement of serotonergic p38alpha mitogen-activated protein kinase for peripheral immune system activation of CNS serotonin uptake and serotonin-linked behaviors. Transl Psychiatry 5 (11):e671. doi:10.1038/tp.2015.168 [PubMed: 26529424]
93. Gourab K, Schmit BD, Hornby TG (2015) Increased Lower Limb Spasticity but Not Strength or Function Following a Single-Dose Serotonin Reuptake Inhibitor in Chronic Stroke. Arch Phys Med Rehabil 96 (12):2112–2119. doi:10.1016/j.apmr.2015.08.431 [PubMed: 26376447]
94. Gurel V, Lins J, Lambert K, Lazauski J, Spaulding J, McMichael J (2015) Serotonin and Histamine Therapy Increases Tetanic Forces of Myoblasts, Reduces Muscle Injury, and Improves Grip Strength Performance of Dmd(mdx) Mice. Dose Response 13 (4):1559325815616351. doi:10.1177/1559325815616351 [PubMed: 26740813]
95. Malinauskaite L, Quick M, Reinhard L, Lyons JA, Javitch JA, Nissen P (2015) HHS Public Access. 21 (11):1006–1012. doi:10.1038/nsmb.2894.A
96. Bermingham DP, Blakely RD (2016) Kinase-dependent Regulation of Monoamine Neurotransmitter Transporters. Pharmacol Rev 68 (4):888–953. doi:10.1124/pr.115.012260 [PubMed: 27591044]
97. Coleman JA, Green EM, Gouaux E (2016) X-ray structures and mechanism of the human serotonin transporter. Nature 532 (7599):334–339. doi:10.1038/nature17629 [PubMed: 27049939]
98. Wang Q, Bubula N, Brown J, Wang Y, Kondev V, Vezina P (2016) PKC phosphorylates residues in the N-terminal of the DA transporter to regulate amphetamine-induced DA efflux. Neurosci Lett 622:78–82. doi:10.1016/j.neulet.2016.04.051 [PubMed: 27113203]
99. Ye R, Quinlan MA, Iwamoto H, Wu H-H, Green NH, Jetter CS, McMahon DG, Veestra-VanderWeele J, Levitt P, Blakely RD (2016) Physical Interactions and Functional Relationships of Neuroligin 2 and Midbrain Serotonin Transporters. Front Synaptic Neurosci 7:20–20. doi:10.3389/fnsyn.2015.00020 [PubMed: 26793096]
100. Zhang YW, Turk BE, Rudnick G (2016) Control of serotonin transporter phosphorylation by conformational state. Proc Natl Acad Sci U S A 113 (20):E2776–2783. doi:10.1073/pnas.1603282113 [PubMed: 27140629]
101. Horvath GA, Meisner L, Selby K, Stowe R, Carleton B (2017) Improved strength on 5-hydroxytryptophan and carbidopa in spinal cord atrophy. J Neurol Sci 378:59–62. doi:10.1016/j.jns.2017.04.047 [PubMed: 28566180]
102. Muller CL, Anacker AM, Rogers TD, Goeden N, Keller EH, Forsberg CG, Kerr TM, Wender C, Anderson GM, Stanwood GD, Blakely RD, Bonnin A, Veenstra-VanderWeele J (2017) Impact of Maternal Serotonin Transporter Genotype on Placental Serotonin, Fetal Forebrain Serotonin, and Neurodevelopment. Neuropsychopharmacology 42 (2):427–436. doi:10.1038/npp.2016.166 [PubMed: 27550733]
103. Robson MJ, Quinlan MA, Margolis KG, Gajewski-Kurdziel PA, Veenstra-VanderWeele J, Gershon MD, Watterson DM, Blakely RD (2018) p38alpha MAPK signaling drives pharmacologically reversible brain and gastrointestinal phenotypes in the SERT Ala56 mouse. Proc Natl Acad Sci U S A 115 (43):E10245–E10254. doi:10.1073/pnas.1809137115 [PubMed: 30297392]
104. Brindley RL, Bauer MB, Walker LA, Quinlan MA, Carneiro AMD, Sze JY, Blakely RD, Currie KPM (2019) Adrenal serotonin derives from accumulation by the antidepressant-sensitive serotonin transporter. Pharmacol Res 140:56–66. doi:10.1016/j.phrs.2018.06.008 [PubMed: 29894763]
105. Coleman JA, Yang D, Zhao Z, Wen P-C, Yoshioka C, Tajkhorshid E, Gouaux E (2019) Serotonin transporter-ibogaine complexes illuminate mechanisms of inhibition and transport. Nature 569 (7754):141–145. doi:10.1038/s41586-019-1135-1 [PubMed: 31019304]
106. Heifets BD, Salgado JS, Taylor MD, Hoerbelt P, Cardozo Pinto DF, Steinberg EE, Walsh JJ, Sze JY, Malenka RC (2019) Distinct neural mechanisms for the prosocial and rewarding properties of MDMA. Sci Transl Med 11 (522):659466–659466. doi:10.1126/scitranslmed.aaw6435

107. Quinlan MA, Krout D, Katamish RM, Robson MJ, Nettesheim C, Gresch PJ, Mash DC, Henry LK, Blakely RD (2019) Human Serotonin Transporter Coding Variation Establishes Conformational Bias with Functional Consequences. ACS Chem Neurosci 10 (7):3249–3260. doi:10.1021/acschemneuro.8b00689 [PubMed: 30668912]

108. Quinlan MA, Robson MJ, Ye R, Rose KL, Schey KL, Blakely RD (2020) Ex vivo Quantitative Proteomic Analysis of Serotonin Transporter Interactome: Network Impact of the SERT Ala56 Coding Variant. Front Mol Neurosci 13:89. doi:10.3389/fnmol.2020.00089 [PubMed: 32581705]

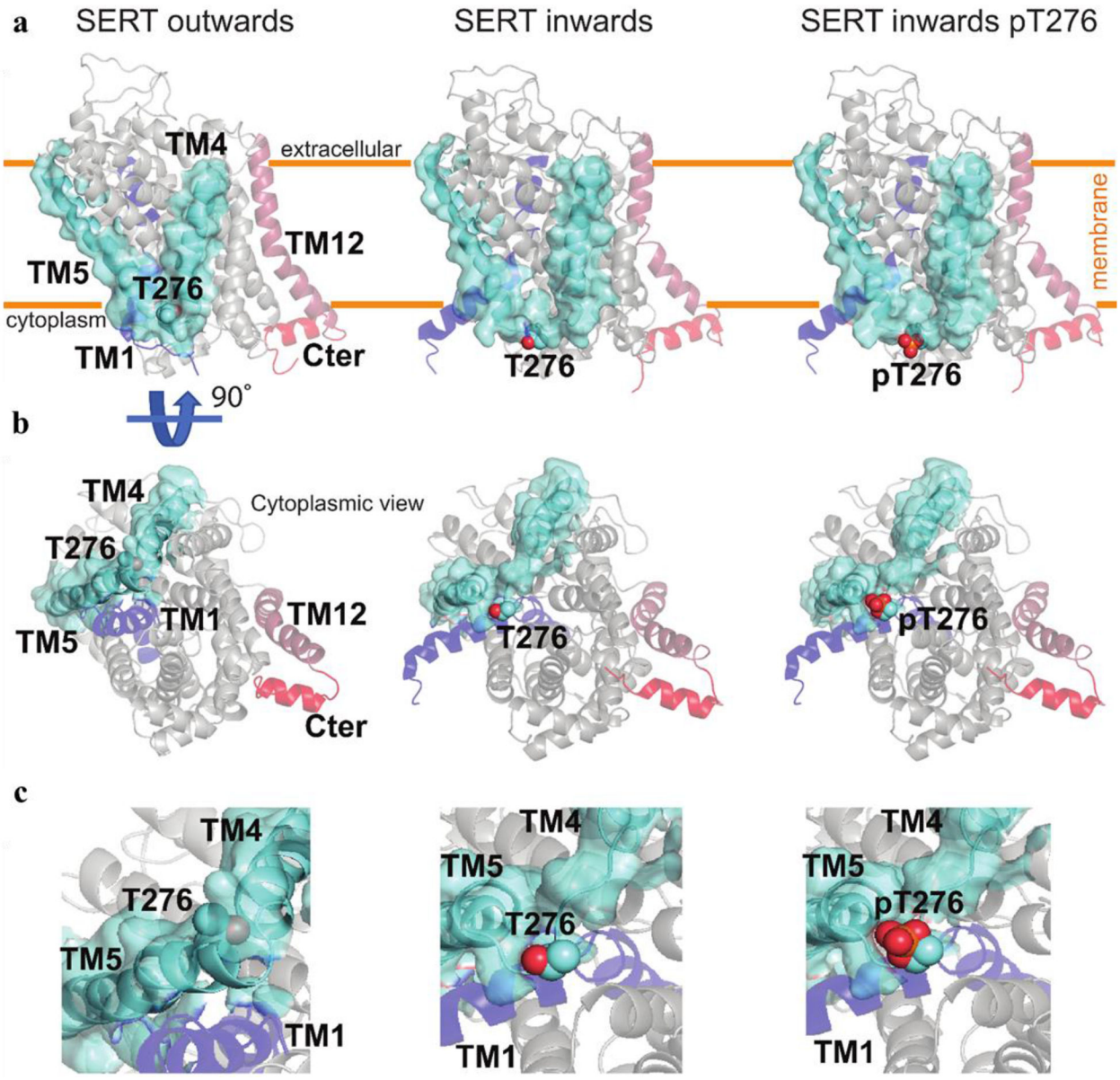

Fig. 1. Transmembrane structures hSERT in outward- and inward-facing conformations illustrating Thr276, the Ala276 substitution and pThr276

(a) Side, **(b)** cytoplasmic and **(c)** cytoplasmic views of hSERT transmembrane domains in outward, WT (left), inward, WT (center) and hSERT pThr276 inward-facing conformations (right). The hSERT in outward-facing conformation corresponds to a structural model obtained using the X-ray structure of hSERT bound to s-citalopram, PDB id: 5I71 [97], as a template. The template-based modelling protocol was used to reverse the mutations found in the X-ray structure 5I67 that did not correspond to the WT hSERT amino acid sequence. hSERT in inwards corresponds the CryoEM structure of hSERT bound to ibogaine (PDB id: 6dzz [105]), whereas pT276 hSERT in inward-facing conformation was obtained after adding a phosphate group to Thr276 in CryoEM 6dzz with Pymol. In all cases, the TM helices are noted in blue (TM1), gray (TM2-3 and TM6-11), cyan (TM4-5), dark red (TM12) and red (C-terminal domain). In addition, TM4 and TM5 are also shown as surface

and Thr276 and pThr276 side chain atoms are shown in spheres. In the outward-facing conformation, Thr276 side chains take part in the packing of the protein with the side chain inaccessible to the solvent in a helical segment. In contrast, in the inward-facing conformation, the same residue is completely exposed to the solvent and is in a coiled (unfolded) segment, similar to pThr276.

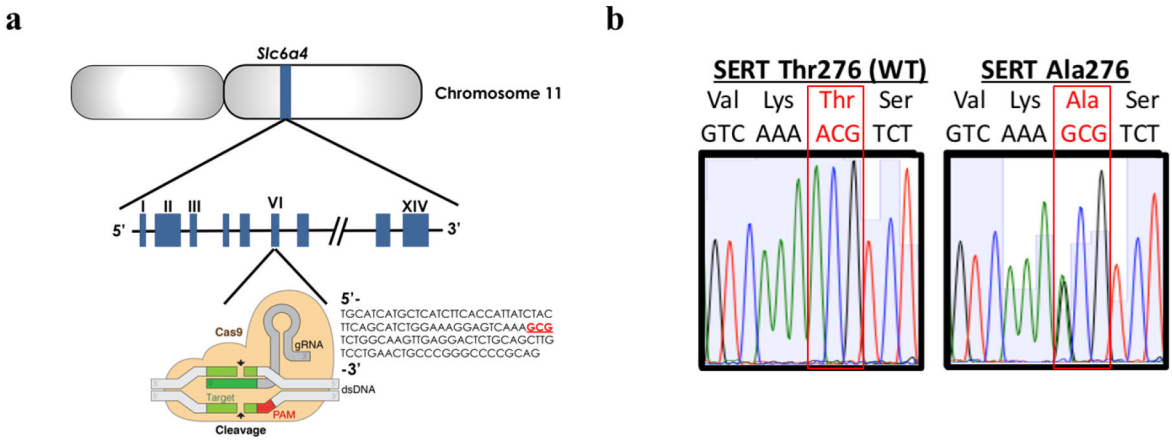

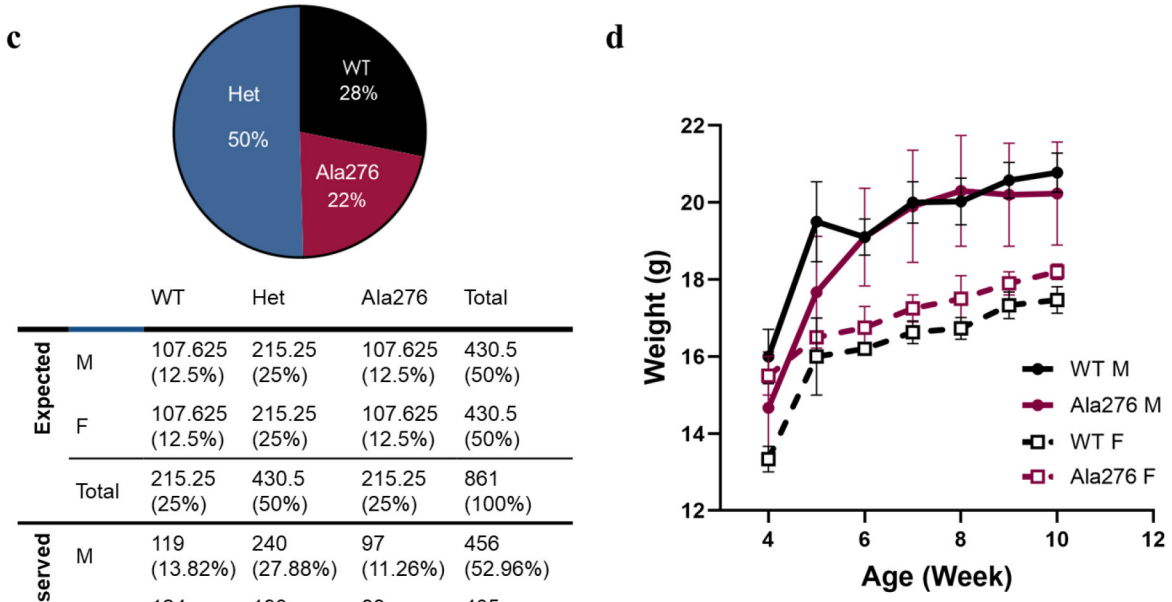

		WT	Het	Ala276	Total
Expected	M	107.625 (12.5%)	215.25 (25%)	107.625 (12.5%)	430.5 (50%)
	F	107.625 (12.5%)	215.25 (25%)	107.625 (12.5%)	430.5 (50%)
	Total	215.25 (25%)	430.5 (50%)	215.25 (25%)	861 (100%)
Observed	M	119 (13.82%)	240 (27.88%)	97 (11.26%)	456 (52.96%)
	F	124 (14.04%)	193 (22.42%)	88 (10.22%)	405 (47.04%)
	Total*	243 (28.22%)	433 (50.29%)	185 (21.49%)	861 (100%)

Fig. 2. Generation of SERT Ala276 mice, genotype distribution and growth assessment

(a) SERT Ala276 mice were generated by a CRISPR/Cas9 approach utilizing a guide RNA targeted against the 6th exon of *Slc6a4* with a donor oligonucleotide that altered an ACG codon encoding Thr to GCG encoding Ala at amino acid 276 **(b)** DNA sequencing of the founder mouse showing a heterozygous genotype with the wildtype ACG overlapped with GCG sequence **(c)** SERT Ala276 show a deviation from the Hardy-Weinberg equilibrium from heterozygous breeders (χ^2 test, genotype effect $^*P < 0.019$); SERT Ala276 mice show normal Mendelian genetics (χ^2 test, male vs. female not significant) **(d)** SERT Ala276 and mice show normal body weights compared to WT mice measured from 4 to 10 weeks (two-way RMANOVA , not significant; n=3-5)

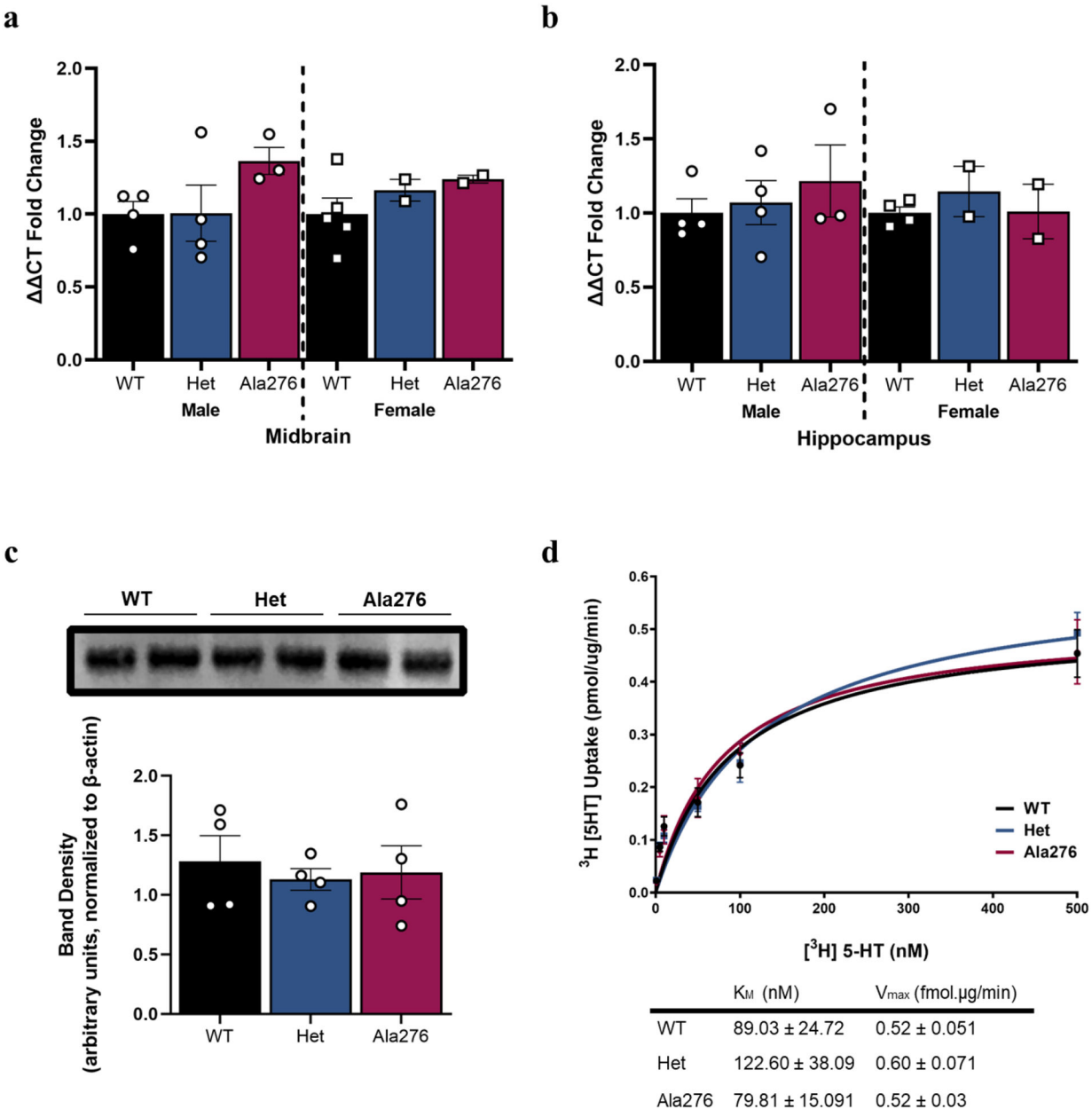

	K_M (nM)	V_{max} (fmol.µg/min)
WT	89.03 ± 24.72	0.52 ± 0.051
Het	122.60 ± 38.09	0.60 ± 0.071
Ala276	79.81 ± 15.091	0.52 ± 0.03

Fig. 3. SERT mRNA, protein levels, and 5-HT uptake kinetics in SERT Ala276 mutant mice

(a) qPCR analysis reveals no significant difference in mRNA levels between genotypes in the midbrain in males and females (one-way ANOVA; midbrain males $P = 0.21$; midbrain females $P = 0.39$; n= 2-5) **(b)** qPCR analysis reveals no significant difference in mRNA levels between genotypes in the hippocampus in males and females (one-way ANOVA; hippocampus males $P = 0.66$; hippocampus females $P = 0.62$; n= 2-4) **(c)** Midbrain SERT protein expression and quantification of SERT protein levels normalized to β-actin reveal no difference in males and females (data combined) across genotypes (one-way ANOVA; P = 0.85; n= 4) **(d)** ^{3}H 5-HT uptake kinetic analysis shows no difference in SERT mediated uptake in males and females (data combined) between genotypes as assessed by both V_{max} and K_M (one-way ANOVA, P>.05, n=5)

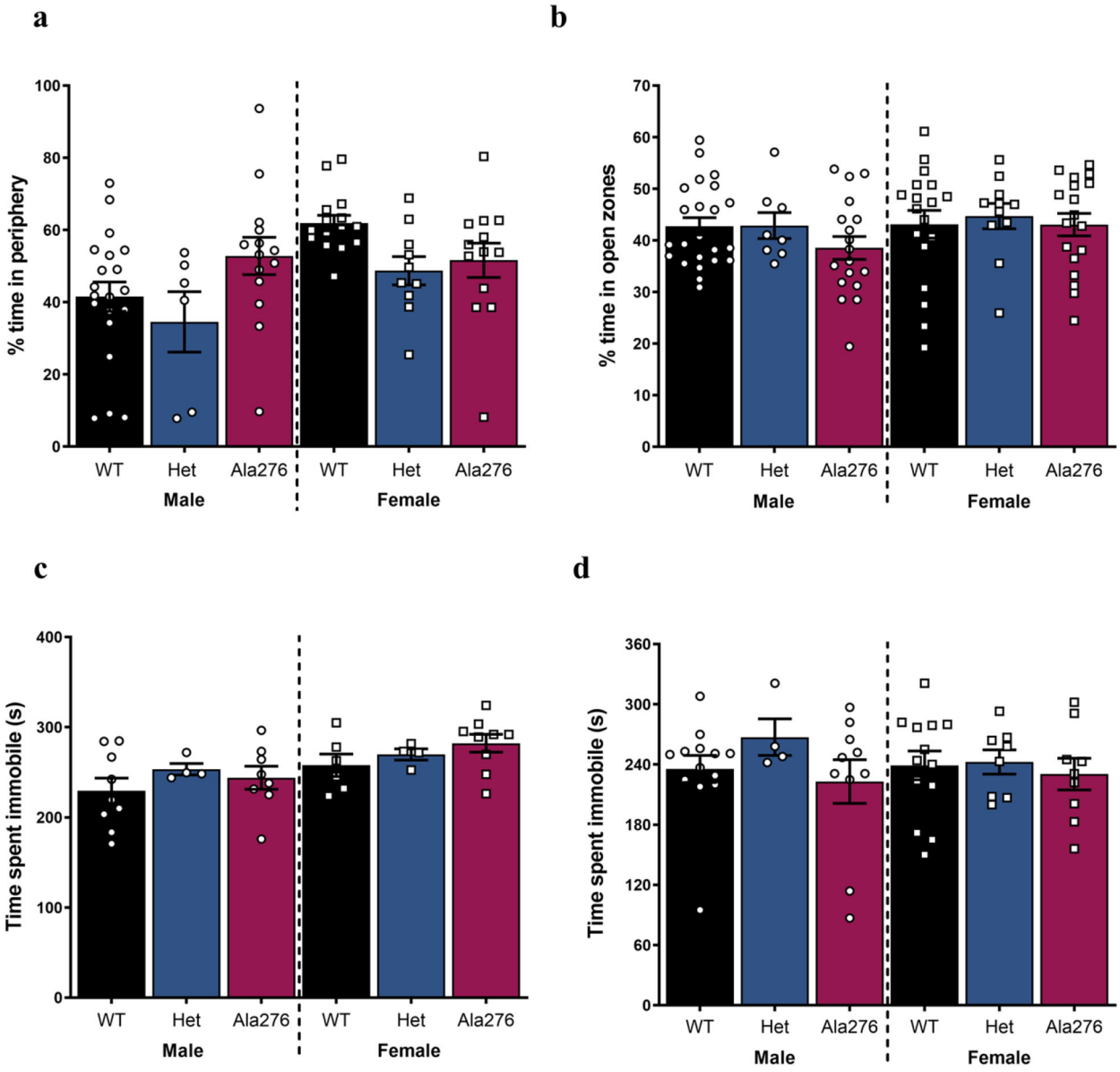

Fig. 4. Normal anxiety and depressive-like behaviors in SERT Ala276 mice

(a) Open field periphery: SERT Ala276 mice spend similar percent of time in the periphery of the open field chamber (One-way ANOVA $P>.05$; n=6-20) **(b)** Elevated zero maze: There is no difference in time SERT Ala276 mice spend in the open arms of the elevated zero maze compared to WT littermate (One-way ANOVA n..s; n=8-23) **(c)** Tail suspension test: Time spend immobile in TST was not different between genotypes for both males and females (One-way ANOVA n..s; n=4-9) **(d)** Forced swim test: Time spend immobile in FST was not different between genotypes for males and females (One-way ANOVA n..s; n=4-13)

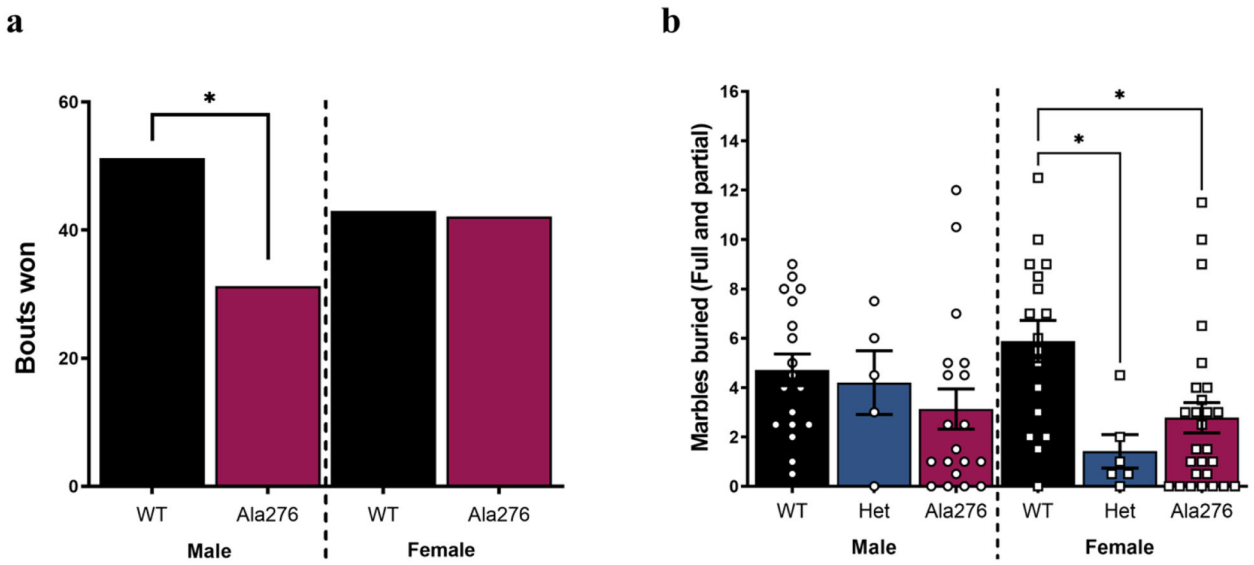

Fig. 5. Sex-dependent effects of SERT Ala276 genotype in tube test and marble burying

(a) Tube Test: In an assessment of social interaction, male SERT Ala276 won less in the tube test compared to WT littermate (χ^2 test *p<0.05; 80 bouts, n=10-15) **(b)** Marble Burying: Female SERT Ala276 heterozygous and homozygous mice bury less marbles in 20 minutes compared to WT female mice (one-way ANOVA followed by Tukey's multiple comparisons test, *$P < 0.05$, n= 5-27)

Table 1

Evaluation of genotype-dependent changes in gross appearance, sensorimotor function and behavior

An Irwin screen conducted as described in Methods revealed no gross abnormalities associated with the SERT Ala276 substitution in either male or female mice. Data from each measure were analyzed by Kruskal-Wallis test, $P > 0.05$, n.s. (n= 6-14)

		WT		HET		Ala276	
		Male	Female	Male	Female	Male	Female
	Sample Size (n)	14	11	6	7	9	6
Physical Factors and Gross Appearance	Body Weight (g)	24.56 ± 0.89	19.05 ± 0.38	24.58 ± 1.63	18.74 ± 0.64	22.97 ± 0.97	17.37 ± 0.92
	Presence of Whiskers	Score 3: 14/14	Score 3: 11/11	Score 3; 6/6	Score 3: 7/7	Score 3: 9/9	Score 3: 6/6
	Appearance of fur	Score 2: 14/14	Score 2: 11/11	Score 2: 6/6	Score 2: 7/7	Score 2: 9/9	Score 2: 6/6
	Piloerection	Score 1: 7/14	Score 1: 5/11	Score 1: 3/6	Score 1: 5/7	Score 1: 5/9	Score 1: 5/6
	Fur missing on face	Score 2; 1/14	Score 2; 0/11	Score 2: 0/6	Score 2: 0/7	Score 2: 0/9	Score 2: 0/6
	Fur missing on body	Score 2: 0/14	Score 2: 0/11	Score 2: 0/6	Score 2: 0/7	Score 2: 0/9	Score 2: 0/6
	Wounds	Score 4: 0/14	Score 4: 0/11	Score 4: 0/6	Score 4: 0/7	Score 4 0/9	Score 4: 0/6
Observation of Behavior in Novel Environment	Transfer Behavior	Score 5: 14/14	Score 5; 11/11	Score 5: 6/6	Score 5; 7/7	Score 5: 9/9	Score 5: 6/6
	Body position	Score 4: 14/14	Score 4: 11/11	Score 4: 6/6	Score 4: 7/7	Score 4 9/9	Score 4: 6/6
	Spontaneous activity	Score 2: 3/14 Score 3:11/14	Score 3: 11/11	Score 2:1/6 Score 2.5: 2/6 Score 3: 3/6	Score 2: 1/7 Score 3: 6/7	Score 2.5: 1/9 Score 3: 8/9	Score 2: 2/6 Score 3: 4/6
	Respiration Rate	Score 2: 14/14	Score 2: 11/11	Score 2: 6/6	Score 2: 7/7	Score 2: 9/9	Score 2: 6/6
	Tremor	Score 2: 0/14	Score 2: 0/11	Score 2: 0/6	Score 2: 0/7	Score 2: 0/9	Score 2: 0/6
	Palpebral closure	Score 2: 0/14	Score 2: 0/11	Score 2: 0/6	Score 2: 0/7	Score 2: 0/9	Score 2: 0/6
	Piloerection	Score 1: 0/14	Score 1: 0/11	Score 1: 0/6	Score 1: 0/7	Score 1: 0/9	Score 1: 0/6
	Gait	Score 0: 14/14	Score 0; 11/11	Score 0: 6/6	Score 0: 7/7	Score 0: 9/9	Score 0: 6/6
	Pelvic elevation	Score 2: 14/14	Score 2: 11/11	Score 2: 6/6	Score 2: 7/7	Score 2: 9/9	Score 2: 6/6
	Tail elevation	Score 1: 14/14	Score 1: 11/11	Score 1: 6/6	Score 1: 7/7	Score 1: 9/9	Score 1: 6/6
	Urination	Score 1: 14/14	Score 1: 11/11	Score 1: 6/6	Score 1: 7/7	Score 1: 9/9	Score 1: 6/6
	Defecation	3	3	2	2	4	3

		WT		HET		Ala276	
		Male	Female	Male	Female	Male	Female
	Sample Size (n)	**14**	**11**	**6**	**7**	**9**	**6**
Reflexes & Reactions to Simple Stimuli	Touch escape	Score 2: 14/14	Score 2; 11/11	Score 2: 6/6	Score 2: 7/7	Score *2.* 9/9	Score 2: 6/6
	Positional Passivity	Score 0: 14/14	Score 0: 11/11	Score 0: 6/6	Score 0: 7/7	Score 0: 9/9	Score 0: 6/6
	Trunk curl	Score 1: 14/14	Score 1: 11/11	Score 1: 6/6	Score 1: 7/7	Score 1: 9/9	Score 1: 6/6
	Body tone	Score 1: 14/14	Score 1; 11/11	Score 1: 6/6	Score 1: 7/7	Score 1: 9/9	Score 1: 6/6
	Pinna reflex	Score 1: 14/14	Score 1: 11/11	Score 1; 6/6	Score 1: 7/7	Score 1: 9/9	Score 1: 6/6
Behavior Recorded During Supine Restraint	Skin color	Score 1: 14/14	Score 1: 11/11	Score 1: 6/6	Score 1: 7/7	Score 1: 9/9	Score 1: 6/6
	Heart rate	Score 1: 14/14	Score 1; 11/11	Score 1: 6/6	Score 1: 7/7	Score 1: 9/9	Score 1: 6/6
	Abdominal tone	Score 1: 14/14	Score 1: 11/11	Score 1: 6/6	Score 1: 7/7	Score 1: 9/9	Score 1: 6/6
	Provoked biting	Score 1: 8/14	Score 1: 5/11	Score 1: 1/6	Score 1: 2/7	Score 1: 4/9	Score 1: 0/6

Table 2

Biogenic amine and amino acid neurotransmitters and metabolites in homozygous SERT Thr276 and SERT Ala276 mice

(a) HPLC assays of tissue content from midbrain and hippocampus as well as **(b)** frontal cortex and cerebellum were performed as described in Methods. No genotype differences were observed ($P > 0.05$, Student's t-test for each sex and region).

a		Midbrain				Hippocampus			
Sex		**Male**		**Female**		**Male**		**Female**	
Genotype		**WT**	**KI**	**WT**	**KI**	**WT**	**KI**	**WT**	**KI**
Sample Size		**7**	**4**	**6**	**4**	**7**	**4**	**6**	**4**
Biogenic amine (ng/mg of protein)	5-HTE	24.64± 0.70	25.25± 6.40	32.83± 1.07	31.12± 1.83	19.57± 1.04	15.05± 3.79	21.01± 0.88	22.10± 2.11
	5-HIAA	14.24± 0.56	15.03± 0.54	17.95± 0.85	22.00± 3.03	7.90± 0.39	7.40± 0.83	9.11± 0.44	11.65± 1.60
	HVA	1.84 ± 0.16	2.19 ± 0.12	2.50 ± 0.13	2.36 ± 0.47	0.76 ± 0.07	0.81 ± 0.19	0.81 ± 0.08	1.29 ± 0.43
	DA	1.53 ± 0.10	1.90 ± 0.35	2.34 ± 0.21	1.75 ± 0.27	0.36 ± 0.07	0.26 ± 0.03	0.23 ± 0.02	0.49 ± 0.19
	DOPAC	1.06 ± 0.08	1.25 ± 0.13	1.41 ± 0.13	1.41 ± 0.22	0.32 ± 0.03	0.34 ± 0.08	0.28 ± 0.03	0.49 ± 0.15
	NE	14.8 ± 0.46	16.97 ± 1.25	16.51 ± 0.58	16.93 ± 1.22	11.43 ± 0.57	12.7 ± 0.83	12.16 ± 0.47	14.14 ± 1.13
	GABA	66.81 ± 1.38	69.07 ± 2.35	72.5 ± 11.4	66.52 ± 1.68	34.85 ± 1.87	36.27 ± 1.51	40.09 ± 1.20	49.28 ± 5.98
	Glutamate	184.80 ± 8.51	204.60 ± 6.96	196.4 ± 7.92	210.80 ± 4.21	228.20 ± 20.3	237.50 ± 15.56	268.30 ± 15.25	291.50 ± 32.29

b		Frontal Cortex				Cerebellum			
Sex		**Male**		**Female**		**Male**		**Female**	
Genotype		**WT**	**KI**	**WT**	**KI**	**WT**	**KI**	**WT**	**KI**
Sample Size		**7**	**4**	**6**	**4**	**7**	**4**	**6**	**4**
Biogenic amine (ng/mg of protein)	5-HT	17.56 ± 0.79	14.38 ± 3.02	17.10 ± 0.99	15.00 ± 1.08	5.63 ± 0.54	5.01 ± 1.82	5.38 ± 0.43	12.43 ± 4.16
	5-HIAA	4.43 ± 0.21	4.79 ± 0.63	4.78 ± 0.42	6.04 ± 0.64	3.01 ± 0.31	2.67 ± 0.57	3.45 ± 0.16	7.77 ± 3.13
	HVA	6.372 ± 0.83	5.98 ± 2.62	6.37 ± 0.83	5.98 ± 2.62	0.34 ± 0.02	0.32 ± 0.04	0.32 ± 0.03	0.69 ± 0.27
	DA	53.77 ± 8.22	37.39 ± 9.48	43.88 ± 5.13	26.59 ± 17.77	0.25 ± 0.01	0.23 ± 0.02	0.24 ± 0.03	0.35 ± 0.05
	DOPAC	5.55 ± 0.74	5.46 ± 1.45	4.42 ± 0.53	4.09 ± 2.16	0.23 ± 0.02	0.18 ± 0.04	0.25 ± 0.02	0.39 ± 0.11
	NE	10.10 ± 0.28	12.41 ± 1.37	10.45 ± 0.24	11.37 ± 0.77	10.45 ± 0.32	11.17 ± 0.63	11.65 ± 0.58	15.36 ± 2.31
	GABA	33.02 ± 1.22	28.68 ± 4.74	32.73 ± 1.15	37.70 ± 1.97	29.40 ± 2.72	25.99 ± 0.80	27.29 ± 1.19	31.38 ± 2.27
	Glutamate	248.90 ± 12.48	258.30 ± 10.15	236.70 ± 4.61	274.60 ± 29.65	161.50 ± 32.83	214.50 ± 13.43	211.90 ± 9.66	205.1 ± 10.8